**Atmospheric
Chemistry
and Physics
Discussions**

Modeling organic aerosols during MILAGRO: application of the CHIMERE model and importance of biogenic secondary organic aerosols

A. Hodzic[1], J. L. Jimenez[2], S. Madronich[1], A. C. Aiken[2], B. Bessagnet[3],
G. Curci[4], J. Fast[5], J. F. Lamarque[1], T. B. Onasch[6], G. Roux[1], and I. M. Ulbrich[2]

[1]National Center for Atmospheric Research, Boulder, CO, USA
[2]University of Colorado, Boulder, CO, USA
[3]Inst. Natl. Environm. Ind. & Risques, INERIS, 60550 Verneuil en Halatte, France
[4]Universita' degli Studi dell'Aquila, Italy
[5]Pacific Northwest National Laboratory, Richland, WA, USA
[6]Aerodyne Research, MA, USA

Full Screen / Esc

Printer-friendly Version

Interactive Discussion

Full Screen / Esc

Printer-friendly Version

Interactive Discussion

Abstract

The meso-scale chemistry-transport model CHIMERE is used to assess our understanding of major sources and formation processes leading to a fairly large amount of organic aerosols (OA, including primary OA (POA) and secondary OA (SOA)) observed in Mexico City during the MILAGRO field project (March 2006). Chemical analyses of submicron aerosols from aerosol mass spectrometers (AMS) indicate that organic particles found in the Mexico City basin contain a large fraction of oxygenated organic species (OOA) which have strong correspondence with SOA, and that their production actively continues downwind of the city. The SOA formation is modeled here by the one-step oxidation of anthropogenic (i.e. aromatics, alkanes), biogenic (i.e. monoterpenes and isoprene), and biomass-burning SOA precursors and their partitioning into both organic and aqueous phases. The near-surface model evaluation shows that predicted OA correlates reasonably well with measurements during the campaign, however it remains a factor of 2 lower than the measured total OA. Fairly good agreement is found between predicted and observed POA within the city suggesting that anthropogenic and biomass burning emissions are reasonably captured. Consistent with previous studies in Mexico City, large discrepancies are encountered for SOA, with a factor of 2–10 model underestimate. When only anthropogenic SOA precursors were considered, the model was able to reproduce within a factor of two the sharp increase in SOA concentrations during the late morning at both urban and near-urban locations but the discrepancy increases rapidly later in the day, consistent with previous results, and is especially obvious when the column-integrated SOA mass is considered instead of the surface concentration. The increase in the missing SOA mass in the afternoon coincides with the sharp drop in POA suggesting a tendency of the model to excessively evaporate the freshly formed SOA. Predicted SOA concentrations in our base case were extremely low when photochemistry was not active, especially overnight, as the SOA formed in the previous day was mostly quickly advected away from the basin. These nighttime discrepancies were not significantly reduced when greatly en-

hanced partitioning to the aerosol phase was assumed. Model sensitivity results suggest that observed nighttime SOA concentrations are strongly influenced by a regional background SOA ($\sim$1.5 μg/m^3) of biogenic origin which is transported from the coastal mountain ranges into the Mexico City basin. The relative contribution of biogenic SOA to monthly mean modeled SOA levels is estimated to be more than 30% within the city and up to 65–90% at the regional scale (even in the immediate vicinity of the city) which may help explain the significant amount of modern carbon in the aerosols inside the city during low biomass burning periods. The anthropogenic emissions of isoprene and its nighttime oxidation by NO$_3$ were also found to enhance the SOA mean concentrations within the city by an additional 15%. Our results confirm the large underestimation of the SOA production by traditional models in polluted regions (estimated as 10–20 Tons within the Mexico City metropolitan area during the daily peak), and emphasize for the first time the role of biogenic precursors in this region, indicating that they cannot be neglected in modeling studies.

1 Introduction

There is growing evidence that organic aerosols affect climate (IPCC, 2007) and human health (Dockery et al., 1992) in proportions that are at present underestimated. Recently, carbonaceous matter has been identified as one of the two largest components of fine particles (together with sulfate) over many continental regions of the Northern Hemisphere, including North America, Europe, and East Asia as well as on the free troposphere (Murphy et al., 2006; Zhang et al., 2007; Yttri et al., 2007). OA is composed of both primarily emitted compounds such as hydrocarbons and fatty acids, and also of chemically processed organic material (i.e. SOA) most of which is water-soluble (Kondo et al., 2007; Docherty et al., 2008). OA-containing particles actively contribute to aerosol radiative forcing by scattering and absorbing solar radiation, and by acting as condensation nuclei for cloud formation (Facchini et al., 1999). In addition, OA contains primary species such as polycyclic aromatic hydrocarbons (Marr et

al., 2006) and secondary species such as quinones (Tao et al., 2003) that have been recognized as highly toxic for human health. Despite their abundance in the troposphere and their adverse effects, organic aerosols are currently the least characterized species of all fine aerosol components in terms of both their chemical composition and spatial distribution. This characterization is all the more challenging as organic aerosol is a complex mixture of hundreds of chemically active individual compounds (Murphy, 2005) among which many have not yet been identified. Hamilton et al. (2004) identified more than ten thousand compounds in an OA sample from London, UK.

The molecular-level identity of the majority of the OA mass is unknown (Turpin et al., 2000). For instance, gas chromatography-mass spectroscopy (GC/MS) can identify the species that comprise only 10–20% of the organic mass. On the other hand the total OA mass can be measured with reasonable accuracy (+/−25%) using thermal-optical analyzers (Turpin et al., 2000) or aerosol mass spectrometers (AMS; Canagaratna et al., 2007). The latter technique has high time and size resolution and allows some characterization of the sources and types of species that make up the total mass through factor analysis of the organic spectrum (Zhang et al., 2005a, b). In particular the total POA and SOA and several subtypes of each have been identified in multiple studies using this technique (e.g. Zhang et al. 2005a, b, 2007; Lanz et al., 2007; Nemitz et al., 2008; Ulbrich et al., 2009). There have been very few measurements that allow a direct estimation of the relative contribution of anthropogenic and biogenic precursors to the SOA formation and the uncertainties are still significant (e.g. Williams et al., 2007; Kleindienst et al., 2007).

Climate and air quality models often underpredict the measured concentrations of organics in urban and remote areas, mainly because the processes involved in the formation and aging of secondary organic aerosols (SOA) are not well understood (e.g. Zhang et al., 2006). According to the study by Volkamer et al. (2006) this underestimation is a already a factor of 3 shortly after the start of the photochemistry and reaches a factor of 8 in urban areas and increases as the air mass ages when using very conservative (favoring SOA) assumptions in the model. Model comparisons using

Modeling organic aerosols during MILAGRO

A. Hodzic et al.

total OC or OA show lower underestimations, as expected due to the influence of POA and sometimes also due to POA overestimation (de Gouw and Jimenez, 2009). These poor modeling results translate into large uncertainties on estimated global production of secondary organic aerosols (70–205 TgC yr^{-1}; Hallquist et al., 2008) as well as on their contribution to aerosol indirect radiative forcing that was qualified as an area of "low level of understanding" by IPCC (2007).

The modeling of SOA formation and aging is currently one of the most challenging and most controversial aspects of aerosol research (Kanakidou et al., 2005; Hallquist et al., 2008). Most 3-D models use a semi-empirical SOA approach (Odum et al., 1996; Pankow, 1994) based on the gas phase oxidation of VOC precursors followed by gas-particle partitioning of two semivolatile products onto existing organic particles depending on local temperature and organic mass concentration. The saturation concentrations of the semivolatile products are derived from fits to measurements from smog chamber experiments of the oxidation of individual VOCs. The effect of temperature on saturation concentration is taken into account using a lumped enthalpy of vaporization (Pun et al., 2003; Donahue et al., 2006). Generally only the lumped first (of early) generation oxidation products from aromatic (e.g. toluene and xylene) and terpene precursors are considered. Only a few models use a more detailed representation of the gas-phase chemistry of SOA precursors while still using lumping and surrogate compounds (Griffin et al., 2002). Fully explicit models have been developed but are too computationally expensive for 3-D applications (e.g. Johnson et al., 2006; Camredon et al., 2007). Several limitations related to these modeling approaches have been discussed in recent studies (Chung and Seinfeld, 2002; Donahue et al., 2006; Simpson et al., 2007; Hallquist et al., 2008; Camredon et al., 2007).

In the past few years, evidence for new precursors and pathways to SOA formation have been identified from measurements including oligomerization (Jang et al., 2002; Kalberer et al., 2004; Iinuma et al., 2004), aqueous-phase production in clouds (Warneck, 2003; Lim et al., 2005), SOA formation from semivolatile and intermediate volatility primary compounds (Robinson et al., 2007), and SOA formation from very

volatile species such as glyoxal (Volkamer et al., 2007). Kroll et al. (2006) and Pun and Seigneur (2007) have shown that species such as isoprene that were previously considered not to form SOA, are likely to act as SOA precursors, and similar findings were recently reported for benzene by Martin-Reviejo and Wirtz (2005) and for acetylene by Volkamer et al. (2008). The nighttime oxidation of isoprene by NO_3 radicals has also been shown to contribute to SOA formation (Ng et al., 2008). A recent chamber based study by Song et al. (2007) suggests that SOA formation from biogenic compounds is insensitive to the presence of hydrophobic primary particles. Their work suggested that the traditional assumption of a well-mixed organic phase (POA+SOA) may be inaccurate, which would have the tendency to artificially enhance model SOA yields.

Improved SOA modules that integrate these recent advances are under development and need extensive evaluation against chamber and ambient aerosol data. Assessment of the significance of some of the above mentioned SOA formation pathways (including the role of biogenic isoprene) in an urban polluted environment is precisely one of the objectives of the present modeling study in Mexico City.

Modeling of organic aerosols had suffered for a long time from the limited availability of ambient OA measurements due to their high cost, and to the low sensitivity and time and size resolution of most OA measurement methods (McMurry et al., 2000). The MILAGRO (Megacity Initiative – Local and Global Research Observations) field experiment that took place in Mexico City during March 2006 provides in that perspective a unique dataset to study the formation and evolution of organic aerosols and their precursors (Molina et al., 2008). Extensive measurement of meteorological variables, gaseous and aerosol pollutants and radiative properties were collected at several urban and near-urban sites as well as aboard regional aircraft flights with the purpose of characterizing the chemical nature and spatial extent of the urban plume, and its transformations during the outflow. The study used a large set of advanced OA measurements which recorded OA data with unprecedented time resolution (e.g. 12 s in aircraft for DeCarlo et al., 2008).

Results from both surface and airborne measurements of the aerosol composition

indicate that Mexico City's fine particles are dominated by organic material (e.g. Salcedo et al., 2006; DeCarlo et al., 2008; Aiken et al., 2009a). The box-model study by Volkamer et al. (2006) could only explain 35% (12%) of the observed SOA concentrations in the morning (afternoon) from traditional anthropogenic precursors (mostly aromatics) inside the city during a case study with very low regional influence. Dzepina et al. (2009) have recently revisited that case study and shown that even with updated aerosol yields, traditional precursors fail to explain more than 15% of the observed SOA growth during that case study. Given the high correlation of organic aerosols with CO and HCN, several studies concluded that anthropogenic activities and biomass burning are the main sources of organic aerosols in the Mexico City area. ^{14}C analyses have attributed 30–75% of the total carbonaceous aerosol observed at the city center to "modern" carbon sources (i.e. biomass and agricultural burning activities, vegetation emissions, and urban sources of modern carbon such as food cooking and biofuel use) (Hildemann et al., 1994; Aiken et al., 2009b; Marley et al., 2009), the balance being due to "fossil" carbon (i.e. POA and SOA from the combustion of fossil fuels). The relative importance of "modern" carbon seems to be higher at the near-city location (T1) than within the city (T0) suggesting a larger regional influence of non-fossil OA sources. It is however unclear what proportion of this modern carbon originates from regional biomass burning vs. biogenic SOA vs. urban sources such as food cooking. A potential influence of "hot" sources of ^{14}C which could produce a high bias on measurements of modern carbon in the Mexico City area has recently been suggested (Vay et al., 2009). Inside the city the formation of biogenic SOA appears to be small, e.g. in a box-model framework Volkamer et al. (2006) report that isoprene and terpenes contribute less than 5% to the total VOC-OH reactivity while Dzepina et al. (2009) report that those species account for ~2% of the SOA predicted to form from these biogenic precursors inside the city. Their estimates were however based on measured concentrations of biogenic VOCs within the city for a particular day characterized by very low regional background SOA, and do not preclude a potentially higher regional contribution to SOA during other periods. We are not aware of any studies that have evaluated

the importance of biogenic SOA on the region around Mexico City. However, the high fraction of modern carbon observed even in periods with low biomass burning (Aiken et al., 2009b) provides additional motivation to investigate this topic.

In this study, we use measurements from several Aerodyne Aerosol Mass Spectrometers (AMS) taken at three ground locations in order to evaluate the skill of the urban-scale chemistry-transport model CHIMERE in simulating OA within the Mexico City metropolitan area. The main focus of the study is to investigate the efficiency of various SOA formation pathways represented in the model and to quantify the relative contribution of anthropogenic and biogenic SOA precursors. We compare the measurements to results from Positive Matrix Factorization of AMS spectra (PMF, Ulbrich et al., 2009; Aiken et al., 2009a, b) which allow the quantification of hydrocarbon-like OA (HOA, a chemically-reduced component which is considered a surrogate for urban POA, including sources such as meat cooking), oxygenated OA (OOA, an SOA surrogate), and biomass burning OA (BBOA). Being able to quantify separately the BBOA fraction allows estimating errors related to the modeling of primary organic aerosols from biomass burning that are difficult to predict in models due to large uncertainties in emission factors and the amount of biomass burned (Fast et al., 2009; Aiken et al., 2009b; Zaveri et al., 2008). In particular, small burning activities (i.e. trash and agricultural fires) are not detected by satellites and therefore not accounted in the emissions retrievals (Yokelson et al., 2009).

Because of the great diversity of SOA formation and evolution processes we limit the discussion in this paper to formation processes that control concentrations of organic aerosols within the city (close to the emission sources). The evolution and aging of the organic aerosols in the outflow of the Mexico City plume will be addressed in future studies (Hodzic et al., 2009). The present paper is organized as follows: MILAGRO measurements and model configuration are described in Sects. 2 and 3 respectively. In Sect. 4, the model ability to represent the transport and mixing of pollutants within the city is evaluated by examining meteorological variables and primary emitted pollutants. In Sect. 5, model predictions of primary and secondary OA are assessed against AMS

Modeling organic aerosols during MILAGRO

A. Hodzic et al.

Title Page

Abstract | Introduction

Conclusions | References

Tables | Figures

◀ | ▶

◀ | ▶

Back | Close

Full Screen / Esc

Printer-friendly Version

Interactive Discussion

results, and the relative contribution of the major SOA formation pathways is discussed. Section 6 summarizes the conclusions of the study.

2 Ground observations during the MILAGRO field project

The MILAGRO (Megacity Initiative: Local and Global Research Observations) field project took place in Mexico City in March 2006. During 1 month an extensive set of measurements of meteorological variables, gas and aerosol pollutant concentrations, chemistry and radiation was collected from ground platforms, aircrafts and satellites, and made publicly available through NCAR, NASA, and DOE data portals. The summary of scientific objectives and experimental design is described by Molina et al. (2008). In this section we briefly present characteristics of measurement sites and data sets used in this study. MILAGRO is the largest of a series of international campaigns in and around Mexico City, which also includes IMADA-AVER in 1997 (Edgerton et al., 1999) and MCMA-2003 (Molina et al., 2007).

To evaluate the model results for POA and SOA within the city basin we use AMS measurements of submicron aerosols (approx. PM_1) collected at two supersites (Fig. 1a) at the Instituto Mexicano del Petroleo (designed as T0) and Universidad Technologica de Tecamac (T1). Data collected by the Aerodyne Mobile Laboratory located on an elevated site of Pico Tres Padres (PTP, 900 m above city ground) on the North of Mexico City are also used. The AMS and its calibration and data analysis techniques have been described in detail elsewhere (Canagaratna et al., 2007, and references therein). The AMS at T0 was a high-resolution time-of-flight AMS (DeCarlo et al., 2006) while those at the other two sites were compact time-of-flight versions (Drewnick et al., 2005) which report unit mass resolution data. Detailed analyses and intercomparisons of the AMS data are reported in separate publications (Aiken et al., 2008, 2009a, b; Herndon et al., 2008; Paredes-Miranda et al., 2008; Zheng et al., 2008; Huffman et al., 2009). The data at T0 (Aiken et al., 2009a) were consistent with previous AMS data collected at another urban site during the MCMA-2003 campaign (Salcedo et al.,

2006). The AMS spectra are analyzed with the PMF technique (Paatero and Tapper, 1994) as described by Ulbrich et al. (2009) and Aiken et al. (2009a). The absolute uncertainty of the AMS concentrations is +/−25% and is dominated by the uncertainty in particle collection efficiency, while the relative uncertainty in the separation of PMF
5 components is of the order of 10% (somewhat lower for high resolution data vs. the unit resolution data). It should be noted that AMS data are reported for ambient atmospheric conditions (T&P) for all three sites, as is the model output.

Observed PBL heights were derived by Shaw et al. (2007) from measured vertical gradients in the radio refractive indices and light scattering obtained by radar wind
10 profilers and a lidar, respectively. Uncertainties associated with these retrievals are of the order of a few hundred meters.

In addition to the MIRAGE dataset, model results have also been assessed against surface chemical and meteorological data collected by the RAMA monitoring network. Comparisons were performed at measurement locations (see Fig. 1) for hourly con-
15 centrations of ozone, carbon monoxide, nitrogen oxides and particles as well as meteorological data including surface temperature, relative humidity, wind speed and wind direction.

3 Air quality model CHIMERE

3.1 General model description

20 In order to simulate the formation and transport of major primary, photo-oxidant, and aerosol pollutants over Mexico City, the meso-scale chemistry-transport model CHIMERE is applied. CHIMERE has been widely used in Europe for air quality process studies (e.g. Bessagnet et al., 2004; Hodzic et al., 2004), operational forecasting (http://www.prevair.org) and inverse modeling of emissions (e.g. Konovalov et al.,
25 2007). Although this is the first time it has been applied in a highly polluted megacity-type environment, its performance in simulating aerosols has been demonstrated within

several model inter-comparison studies (e.g. Stern et al., 2008) and field projects (e.g. Hodzic et al., 2006) in Europe. Improving the representation of organic aerosols constitutes one of the major challenges for CHIMERE (Bessagnet et al., 2009). A detailed description of the model is presented in previous references and can also be found on http://euler.lmd.polytechnique.fr/chimere. In this section, we briefly describe the aerosol module and the updates that have been included for the purpose of this study.

Tropospheric photochemistry is represented using the MELCHIOR chemical mechanism (Lattuati, 1997) that includes 120 reactions and 44 prognostic gaseous species. In addition to gaseous pollutants, 10 aerosol components are considered in the present application, including primary organic (POA) and black (BC) carbon, other unspecified primary anthropogenic components, wind-blown dust, secondary inorganics (sulfate, nitrate and ammonium) as well as secondary organic aerosols from anthropogenic and biogenic origin, and particulate water. The size distribution is represented using a sectional distribution, considering 8 size bins geometrically spaced from 40 nm to 10 μm in physical diameter. The thermodynamic partitioning of the inorganic mixture (i.e. sulfate, nitrate, and ammonium) is computed using the ISORROPIA model (Nenes et al., 1998). The dynamical processes influencing aerosol growth such as nucleation, coagulation and absorption of semi-volatile species are included in the model as described by Bessagnet et al. (2004). Heterogeneous chemical processes onto particles and a simplified sulfur aqueous chemistry are also considered. Dry and wet deposition for all gaseous and aerosols species are computed as a function of the friction velocities and stability of the lowest model layer (Wesely, 1989), and as a function of grid-averaged precipitation rates and cloud water content (Tsyro, 2002; Loosmore and Cederwall, 2004), respectively. Clear sky photolysis rates are calculated off-line based on the TUV model (Madronich et al., 1998), and they are modified when in the presence of clouds. The effect of aerosols on photolysis rates is not included (Hodzic et al., 2007).

3.2 SOA formation from anthropogenic and biogenic VOC precursors

Modeling of secondary organic aerosol formation requires (I) a gas-phase mechanism to predict the rate of formation of semivolatile products from the oxidation of VOCs, and (II) a thermodynamic module to predict the gas-particle partitioning of these species. In CHIMERE, SOA formation is represented according to a simplified approach described by Pun et al. (2005, 2006). The performance of this SOA formation mechanism has been assessed mainly against smog chamber data (Pun et al., 2006), and with total daily-averaged OC concentrations in the US (Pun et al., 2003) and Europe (Bessagnet et al., 2009). In the present study, the predicted SOA from CHIMERE will be evaluated for the first time against AMS measurements offering high temporal resolution and some chemical/source resolution.

3.2.1 Gas-phase chemistry of precursors

The MELCHIOR gas-phase mechanism has been extended to account for one-step lumped oxidation of aromatic and biogenic compounds as shown in Table 1 (Pun et al., 2005, 2006; Bessagnet et al., 2009). For anthropogenic compounds, three families of precursors are considered including benzene, toluene and other mono-substituted aromatics (TOL); xylene, tri-methyl-benzene and other poly-substituted aromatics (TMB); and higher alkanes. The gas-phase chemistry (oxidation by OH, O_3 and NO_3) of four biogenic SOA surrogates are considered in this study including α-pinene and sabinene (APIN); β-pinene and δ^3-carene (BPIN); limonene (LIM); ocimene and myrcene (TPO). Day- and nighttime chemistry of isoprene has been added for this study as described below. Other reactive biogenic VOCs such as sesquiterpenes are not considered here because their emissions are highly uncertain. Recent work by Liao et al. (2007) indicated a small contribution of these precursors to SOA formation compared to isoprene and monoterpene, while other studies have reported a comparable contribution to SOA among these three sets of precursors (Kleindienst et al., 2007).

The condensable oxidation products from both anthropogenic and biogenic precur-

sors are lumped into 9 groups of surrogate compounds (i.e. AnA0D, AnA1D, AnA2D, AnBmP, AnBlP, BiA0D, BiA1D, BiA2D, BiBmP) according to their physico-chemical properties including their hydrophobicity, acid dissociation and saturation vapor pressure (see Table 2). As explained by Pun et al. (2006), the physico-chemical properties of surrogate species, such as the molecular weight, are determined based on the structure and functional groups of each surrogate compound. The Henry's law constant and the saturation vapor pressure of the surrogate species are derived from the geometric average property of the group.

In this study all hydrophilic oxidation products (e.g. AnA0D, AnA1D, AnA2D) were grouped into a single surrogate compound (i.e. AnA1D for anthropogenics and BiA1D for biogenics) in order to increase computational efficiency. The stoichiometry coefficient for this product was derived from the sum of the stoichiometry coefficients of individual hydrophilic oxidation products used in the base model presented in Pun et al. (2005, 2006). According to several studies (Griffin et al., 2002; Pun et al., 2003; Varutbangkul et al., 2006; Prenni et al., 2007) based on laboratory experiments, most SOA products present in the particulate phase are not very hydrophilic. Therefore, grouping hydrophilic oxidation products into a single hydrophilic compound (AnA1D for anthropogenic and BiA1D for biogenic species) with moderate saturation vapor pressure characteristics is not expected to greatly impact the predicted SOA mass and seems to be a reasonable assumption in this study.

In this work we assume that all gaseous semi-volatile organic species undergo dry deposition based on Wesely (1989). As the deposition velocities for these species have not yet been determined, deposition velocities have been calculated similar to NO_2. Consideration of dry deposition is expected to lower the predicted SOA concentrations by 10–20% (Bessagnet et al., 2009).

3.2.2 Gas/particle partitioning of condensable material

The gas/particle partitioning is treated as an external mixture of hydrophilic and hydrophobic particles (Pun et al., 2006). Hydrophilic SOA surrogates dissolve into ex-

Modeling organic aerosols during MILAGRO

A. Hodzic et al.

Title Page

Abstract | Introduction

Conclusions | References

Tables | Figures

◄ | ►

◄ | ►

Back | Close

Full Screen / Esc

Printer-friendly Version

Interactive Discussion

isting aqueous particles (associated with the inorganic phase) following Henry's law. Hydrophobic SOA surrogates absorb into organic particles according to equilibrium gas/particle partitioning (Raoult's law) between the aerosol phase and gas phase. The equilibrium concentrations are a function of the particle chemical composition, temperature and relative humidity for hydrophilic species (Pun et al., 2006). Similar to Bessagnet et al. (2009), the mass transfer between gas and aerosol phases is represented by dynamic gas-particle absorption theory for each aerosol size bin. However, unlike in Bessagnet et al. (2009) that used both inorganic and secondary organic aerosol mass for the partitioning of semi-volatile organics to obtain an upper limit of SOA formation, even though equilibrium partitioning of SOA into inorganic aerosols has not been demonstrated experimentally, we use in this study the better justified assumption of semivolatile partitioning into a well-mixed organic phase (POA+SOA). This results in a considerably lower, but presumably more realistic, amount of SOA being formed by the model at the regional scale compared to the model formulation of Bessagnet et al. (2009). In this study POA species are treated as non-volatile.

3.2.3 Additional SOA formation pathways considered in this study

In addition to the SOA module based on Pun et al. (2005, 2006), we consider here two newly recognized SOA formation pathways including the oxidation of isoprene by OH (Henze and Seinfeld, 2006) and the nighttime oxidation of isoprene by nitrate radicals (Ng et al., 2008).

Recently, isoprene has been identified to significantly contribute to SOA formation (e.g. Limbeck et al., 2003; Claeys et al., 2004; Kroll et al., 2006). Henze and Seinfeld (2006) have reported an increase of a factor of 2 in predicted SOA concentrations at the global scale after accounting for SOA formation from isoprene. Within the CHIMERE model, SOA production from isoprene is represented according to the two-product parameterization under low-NOx conditions developed by Henze and Seinfeld (2006) based on experimental data from Kroll et al. (2006). Table 1 presents the first-generation oxidation of isoprene by OH leading to the formation of two semivolatile

products (ISO1 and ISO2) that can be absorbed into aerosols following gas/particle equilibrium partitioning theory (see Table 2).

In addition to the daytime chemistry of isoprene, it has been observed that isoprene mixing ratio drops rapidly after sunset when OH radicals are no longer available (e.g. Stroud et al., 2002). The rapid reaction with nitrate radicals, NO_3, is believed to be the major contributor to isoprene decay at night, leading to the formation of low-volatility products (Ng et al., 2008; Brown et al., 2009). Table 1 presents the reaction of isoprene and NO_3 as it was included into CHIMERE. This first-generation oxidation leads to the formation of two semivolatile reaction products (ISO3 and ISO4) that can further be partitioned to the aerosol phase (Table 2).

3.3 Model configuration and simulation design for MILAGRO

3.3.1 Model setup

CHIMERE baseline and sensitivity simulations are performed locally over the Mexico City area using a one-way nesting procedure where a coarse simulation with a 35 km horizontal resolution over all of Mexico and the North of Central America (Fig. 1) is first carried out. Boundary conditions for this regional simulation are provided by monthly climatology of the LMDZ/INCA global chemistry-transport model (Hauglustaine et al., 2004) for gaseous species and the GOCART model (Ginoux et al., 2001) for aerosol species. Concentrations from this regional simulation are then used every hour to force at the boundaries the higher resolution simulation ($5 \times 5 \, km^2$), performed over a nested grid of Mexico City and surrounding region (Fig. 1). Vertically, terrain following hybrid sigma-pressure coordinates are used including 20 vertical layers, unequally distributed between the ground and the 300 hPa pressure level.

The meteorological input fields are taken from the MM5 mesoscale model (Dudhia et al., 1993). MM5 is initialized and forced at the boundaries by the 6-hourly analyses of the AVN model of the National Centers for

Environmental prediction (NCEP), given on a 1°×1° grid. In order for the model to

stay close to the analyses for this month-long simulation, the nudging option is used above the boundary layer throughout the MM5 model domain for wind and temperature.

3.3.2 Anthropogenic emissions

Anthropogenic emissions for the Mexico City metropolitan area (MCMA) are based on the 2002 official Mexican emission inventory (CAM, 2004). This emission set has already been used and evaluated in previous modeling studies over Mexico City (Lei et al., 2007; Fast et al., 2009). The methodology used to derive spatially and temporarily resolved emissions from total annual quantities reported in the inventory is described by Lei et al. (2007). The total annual emissions of VOCs, CO, NOx and aerosols for various source categories including mobile, area and point sources were transformed into temporally resolved and chemically speciated emission data: (I) the diurnal cycle was applied for all species based on West et al. (2004); (II) the weekend effect was also considered based on traffic count information for CO and resulted in an decrease of total emissions by 10% for Saturdays and 30% for Sundays compared to week-day emissions; (III) the volatile organic compound (VOC) speciation was performed following the procedure described in Velasco et al. (2007). Based on an extensive comparison with the ground observations from the 2003 MCMA field experiment, Lei et al. (2007) have adjusted the emissions for VOC species used in the present inventory to better match the observed values. That resulted in an increase of 65% of the VOC total emitted mass, but with variable adjustment for individual VOCs components. Outside Mexico City we complemented the MCMA emission inventory by the regional NEI 1999 emissions (M. Mena, personal communications, 2007). The description of the inventory can be found at http://mexiconei.blogspot.com/. Fast et al. (2009) suggest that the MCMA inventory is more accurate than the NEI for CO and EC.

Emissions from biomass burning activities are accounted for in the present study with the same procedures as in Fast et al. (2009) and resulting in similar predicted concentrations. Estimates of daily emissions of trace gases and primary particles together with their geographic location were derived from satellite data as described by

Wiedinmyer et al. (2006) and included within the CHIMERE model following Hodzic et al. (2007).

3.3.3 Biogenic emissions

Hourly emissions of nitrogen oxides and eight biogenic VOC species (isoprene, α-pinene, β-pinene, myrcene, sabinene, limonene, δ^3-carene, ocimene) are considered in this study. In the standard configuration of CHIMERE biogenic emissions are calculated using the algorithms of Guenther et al. (1995), combined with emissions factors for European species (e.g. emission potential, foliar density, tree distribution) developed by Simpson et al. (1999). As such characterization of the vegetation is not available for the Mexico City region, biogenic emissions were generated using the global scale model MEGAN (Model of Emissions of Gases and Aerosols from Nature, http://bai.acd.ucar.edu) developed by Guenther et al. (2006). The emission rates are determined as a function of (I) gridded emission factors averaged over local plant functional types (i.e. needleleaf trees, broadleaf trees, shrubs, grass, crops) at standard conditions, and (II) several activity factors that account for variations of environmental conditions with respect to the standard. The driving environmental variables are (I) monthly mean leaf area index (LAI) provided with MEGAN and derived from satellite observations, and (II) ambient temperature and short-wave radiation supplied at hourly rates by the MM5 model. The variation of LAI is used to calculate a leaf-age activity factor, while the other two variables are used to simulate the hourly vegetation response to leaf temperature and photo-synthetically active radiation respectively. The evaluation of the MEGAN model with regard to isoprene emissions has been extremely limited, and mainly based on in-situ flux measurements or satellite data of isoprene reaction products such as formaldehyde. Muller et al. (2008) have reported a reasonable agreement between simulated and measured isoprene fluxes over the Southern US, while Warneke et al. (2009) report a slight overestimation of isoprene from MEGAN over the Eastern US and Texas. For our region of interest, we verified that the spatial distribution of broadleaf trees which is the main emitter of isoprene is consistent

with vegetation types provided by an independent data base (Global Land Cover Facility, GLCF, http://glcfumiacs.umd.edu). In addition, we compared modeled isoprene concentrations with canister-based measurements from the G1 aircraft that were available during MILAGRO (see Supplement http://www.atmos-chem-phys-discuss.net/9/12207/2009/acpd-9-12207-2009-supplement.pdf, Fig. 1). The comparison is limited to the immediate vicinity of Mexico City, and shows that predicted isoprene is of comparable magnitude or lower than the measured values, suggesting that the isoprene emissions are not overestimated in our model. Similar results are also found for ground isoprene values within the city (as discussed in Sect. 5.4). Data are however not available over forest areas in the coastal region where the highest isoprene emissions are predicted by the model (see Fig. 1).

3.3.4 Simulations

For this study, the CHIMERE model is run from 1 to 31 March 2006 for both regional and urban-scale simulations. A 3-day spin-up, from 1 to 3 March, is considered to initialize the model from climatological values and the model predictions for this time period are not used for comparisons with observations. Several model simulations were carried out (see Table 3) in order to determine the relative contribution to SOA formation of various precursor sources including anthropogenic, biogenic and biomass burning emissions, and to evaluate the sensitivity to the gas/particle partitioning parameters. For comparison with measurements, the simulated parameters are spatially and temporally interpolated at the location of the measurement sites. The ground measurements are compared with the model's lowest level (about 25 m above the surface). Only predicted organic aerosols from the lower five size bins (below 1.2 μm in diameter) were considered for the comparison with AMS measurements.

4   Chemical and meteorological conditions

4.1   Synoptic weather during March 2006

Weather conditions during March 2006 were typical of the dry season in Mexico characterized by clear skies, low humidity, and weak winds aloft associated with high-pressure
systems. Afternoon maximum temperatures within the city ranged from 20 to 29°C, and
surface winds were below 5 m/s most of the time (Fig. 2). According to observed wind
regimes, three types of synoptic conditions were distinguished by Fast et al. (2007): (I)
the first regime prior to 14 March was characterized by a high pressure system slowly
moving from northwestern Mexico towards the east associated with northerly and east-
erly synoptic winds over Mexico City. (II) the second regime between 14 and 23 March,
was associated with the passage of a weak cold surge on 14 March, the development
of late afternoon convection, and variable wind directions. The rest of this period was
drier as the deep convection gradually diminished after 18 March and synoptic winds
progressively turned southwest. (III) The third regime after 23 March began with the
passage of a strong cold surge that lead to higher humidity, afternoon convection, and
precipitation over the central plateau. After 25 March, high pressure progressively de-
veloped over southern Mexico associated with westerly winds over central Mexico for
the rest of the month. A detailed overview of meteorological conditions during MILA-
GRO can be found in the overview by Fast et al. (2007).

4.2   Ozone and aerosol surface concentrations during the period

Figure 3 shows average hourly concentrations of O_3 and $PM_{2.5}$ observed by urban
stations of the RAMA network during March 2006. Moderately high ozone levels are
observed during the entire month with ozone peaks generally exceeding 70 ppbv in
the afternoon, except from 18 to 20 March, a period during which peak concentra-
tions remained below average. These three days were associated with stronger winds
both at the surface and aloft (not shown here), causing faster dispersion of pollutants.

Ozone diurnal variability is typical of a photochemically generated pollutant with peak concentrations occurring in the early afternoon (i.e. from 12:00 to 16:00 LT). Evening concentrations decrease significantly and remain very low (<10 ppb) during the night due to titration with fresh NO emissions. Strong day-to-day variability in the spatial distribution of ozone concentrations (also true for other species) is observed during the MILAGRO experiment caused by important changes in the surface circulation patterns.

The $PM_{2.5}$ average concentrations vary from morning peak traffic hour values of $30\,\mu g\,m^{-3}$ to an afternoon peak value of 50–$55\,\mu g\,m^{-3}$. It is clear that aerosol has both primary and secondary influences that lead to a significant increase of the concentrations during the morning rush hour and then a significant mass creation in the late morning by photochemistry. As already noted by Stephens et al. (2008) for PM_{10}, the observed $PM_{2.5}$ evening peak occurs two hours earlier (02:00 UTC i.e. 20:00 LT) than CO and NO_x peaks (04:00 UTC i.e. 22:00 LT), and its temporal occurrence is not well captured by the model. The presence of a large amount of coarse particles (revealed by the difference between PM_{10} and $PM_{2.5}$ observations, not shown) suggests that wind-blown dust is contributing significantly to the aerosol load in the late afternoon (Querol et al., 2008) in addition to remaining high levels of secondary aerosols produced during the daytime. The wind-blown dust is accounted for in the model, and it represents a large fraction of the predicted $PM_{2.5}$ aerosol within the city (contribution ranging from 10% up to 70% on windy days). Background concentrations are maintained over night, most likely the consequence of limited vertical dispersion of primary emissions in a shallow nighttime boundary layer, and of transport of regionally generated pollutants into the basin from surrounding areas late in the day (Moffet et al., 2007).

Unlike for other polluted cities, e.g. Paris (Hodzic et al., 2006) or Pittsburgh (Zhang et al., 2005c), we do not observe strong multi-day accumulation of pollutants within the Mexico City basin during March 2006 despite the fact that the daily production of primary and secondary pollutants is very intense. Although the city is in a basin and is mostly surrounded by mountains, the valley is well ventilated at the end of the day as a

Modeling organic aerosols during MILAGRO

A. Hodzic et al.

Title Page

Abstract | Introduction

Conclusions | References

Tables | Figures

◄ | ►

◄ | ►

Back | Close

Full Screen / Esc

Printer-friendly Version

Interactive Discussion

result of converging thermally-driven circulations (Fast and Zhong, 1998; de Foy et al., 2006) and because it is open to both the north and south (see Sect. 4.3).

4.3 Evaluation of meteorological and chemical simulation

The meteorological variables such as wind speed and planetary boundary layer (PBL) height are essential parameters that control the dispersion and vertical mixing of gaseous and aerosol pollutants. Thus, before evaluating the CHIMERE chemistry-transport model skill to reproduce aerosol pollutant concentrations we first examine whether these meteorological variables are adequately reproduced by the MM5 meteorological model during the period of interest.

Figure 4 shows windroses of observed and modeled winds for each of the 15 available RAMA surface stations. Both model and measurements indicate the occurrence of weak (<5 m/s) and disorganized winds during March 2006 in relation with stagnant atmospheric conditions and valley-type near-surface circulation. The valley's influence on wind direction is clear for stations located at the southwest edge of the city with winds predominantly from the southwest indicative of the down-slope circulation. This southwesterly flow is qualitatively represented by the model. In the eastern part of the basin, surface circulation is dominated by stronger southerly winds (up to 10 m/s) which penetrate the basin in the afternoon through the southeast mountain gap bringing background air from outside the basin (Doran and Zhong, 2000). Modeled southerly flow is more frequent than observed and goes deeper into the basin leading to a higher frequency of southerly winds at four northern stations. This qualitative comparison suggests that the model is capturing the overall features (wind direction and speed) of the near-surface circulation reasonably well.

A more systematic comparison of measured and simulated average wind speed at RAMA sites displayed in Fig. 2b demonstrates the ability of the model to reasonably reproduce the temporal variability of the wind velocity during MILAGRO. On most of the days, predicted wind speed fall into the observational variability interval and the overall model bias is small (0.21 m/s). During the day winds stay relatively weak (~1 m/s)

until late afternoon when they increase significantly (>3 m/s) favoring the dispersion of pollutants.

Figure 2 also shows temporal trends of observed and predicted surface temperature and relative humidity averaged among all RAMA stations. Surface temperature is predicted accurately for the entire period under study. Modeled values stay within the observational variability and are highly correlated with measurements (correlation of 0.97). A slight cold bias of 0.5°C can be noticed mainly at night which is characteristic of the MM5 model (Zhong and Fast, 2003). During March 2006, the observed RH values are adequately reproduced by the model, except for the 5–7 March period where an overestimation of 20–30% RH in predicted values is obtained for nighttime values. Dryer daytime values (10–30%) as well as the increase in humidity toward the end of March seem correctly captured by the model for these surface stations. Verifying the model's ability to reproduce the T and RH is important as these parameters play a determining role in aerosol thermodynamics and chemistry.

Finally, a comparison of the MM5 planetary boundary layer (PBL) height is performed using measurements obtained during MILAGRO. Modeled PBL height was determined from the Richardson number in a similar way as in Troen and Mahrt (1986), based on a critical value (0.5) of the bulk Richardson number, in the MRF PBL scheme. Figure 5a shows time series of observed and predicted PBL heights at the urban site of T0. Observed and simulated PBL height ranges from 2.5 to 4 km during the day. The comparison reveals a slight underestimation of the observed PBL height for a few specific days, but this behaviour is not a persistent bias. Following Fast et al. (2009), the comparison of observed and predicted average diurnal PBL depth profiles provides a better understanding of the model behaviour at T0 and T1. The sharp ascent of the PBL in the late morning seems to occur 1 h earlier in the model than observed. The diagnosing of the PBL height seems to be more challenging for the model during the late afternoon and over night, as the predicted PBL collapses 2 h sooner than observed, and stays significantly lower over night.

The nighttime PBL is especially difficult to model over urban areas as urban canopy

effects are poorly represented in the MM5 model due to the absence of a specific urban canopy model and other factors (like anthropogenic heat fluxes) affecting PBL mixing (Liu et al., 2004; Hodzic et al., 2005). As in Hodzic et al. (2005), a minimum PBL height of 300 m is assumed in this study to prevent unrealistically low nighttime mixing of pollutants. It should also be noted that the comparison at sunset is more uncertain as PBLH retrievals from lidar and wind profiler cannot accurately distinguishing between the top of the residual layer and the shallow inversion layer that develops during this transition period. PBLH measurements from radiosondes confirm this large uncertainty during sunset, and yield 300–1000 m lower PBLH values at T1 site than lidar retrievals. Similar difficulties have also been reported for the WRF model during the MILAGRO experiment (Fast et al., 2009).

Errors in simulated PBL height could generate discrepancies between observed and modeled concentrations of primary pollutants. Such is the case for CO as illustrated in Fig. 3 (see CO average diurnal profile). Indeed, the model underestimation of the PBL height contributes to an erroneous CO peak in the late evening and somewhat high CO values during the morning rush hour peak that are consistent with weaker vertical mixing predicted by the model. However, there is a strong variability in CO concentrations among RAMA stations. Model overestimation during the morning rush hour seems to occur mainly at stations located within the city center (individual comparisons are not shown here), where the urban canopy tends to enhance vertical mixing and lead to better mixed pollutants than at the edges of the city. Besides the underestimated mixing, this location dependency suggests that primary emissions could be slightly overestimated in some parts of the city. Finally, CHIMERE reproduces the CO average temporal fluctuations observed at RAMA stations during March 2006 quite well as indicated by a high correlation coefficient (0.76) shown in Fig. 2.

Systematic comparison of observed and modeled concentrations of O_3, NO_2 and fine particles has also been performed for all available RAMA data during March 2006. Unlike for CO, concentrations of these species are determined not only by primary emissions and mixing, but also photochemical reactions. As shown in Fig. 3, the model

reproduces the surface ozone time variations during March 2006, as indicated by a high correlation coefficient (0.92). CHIMERE reasonably captures the sharp increase in ozone concentrations in the late morning that correspond to the beginning of the photochemical production of ozone. The monthly mean ozone peak concentrations are underestimated by approximately 10% in the model. However, the peak values are within the range of variations among RAMA stations (Fig. 3, gray shadings). In the late afternoon, the predicted ozone concentrations drop more rapidly than observed as a result of a too rapid collapse of the predicted PBL height which enhances the NO titration effect. Overnight, in the absence of sunlight, ozone concentrations stay very low and their magnitude is correctly represented by the model. These results suggest that ozone photochemical production and NO titration as well as ozone background concentrations are correctly simulated by CHIMERE. The model ability to predict ozone chemistry is also confirmed by a good agreement (small positive bias of 1.1 ppb and correlation of 0.78, see Supplement http://www.atmos-chem-phys-discuss.net/9/12207/2009/acpd-9-12207-2009-supplement.pdf, Fig. 2) found between observed and predicted concentrations of oxidant Ox (defined as O_3+NO_2), which is a more conservative species because it is not affected by O_3 titration with NO. Moreover, the evolution of NO_2 concentrations near the surface is rather well captured during this period (correlation of 0.72), except on 17 and 21 March when the model overestimates the observed concentrations by a factor of 3. This discrepancy coincides also with a major CO overprediction and is most likely related to a combination of a too weak dispersion and/or too high emissions at peak traffic hours. In general during anticyclonic conditions characterized by very low winds (∼1 m/s), relatively small errors (a few m/s) in the wind speed can translate into large discrepancies between predicted and observed concentrations.

For PM$_{2.5}$, the model stays on the low side of observed values throughout the day as illustrated in Fig. 3 (see average diurnal profiles), except on the peak of the PBL collapse, consistent with the observations above. Fine particulate matter has major contributions from both primary and secondary species, with SOA representing about

a quarter of the fine PM mass (Salcedo et al., 2006; Volkamer et al., 2006; Aiken et al., 2009a). Although this model run includes SOA chemistry, the model underestimation is expected given the fact that many studies support that SOA formation in current models is insufficient to explain the observed ambient urban SOA levels. Issues related to the SOA formation will be further discussed in Sect. 5.

For both ozone and aerosols, the greatest model underprediction occurs on 10–11 March and 18–20 March. This model error can be caused by exaggerated dispersion of pollutants in the model as suggested by the comparison of observed and predicted wind speed (Fig. 3). Model simulated midday winds are a factor of 2–3 higher during these stagnant days (3 m/s instead of 1 m/s), which has a tendency to unrealistically enhance the horizontal dispersion of pollutants. Fast et al. (2009) have also reported occurrence of large errors in POA predictions related to discrepancies in wind fields (e.g. on March 20). Those days also coincide with high biomass burning activity, characterized by the occurrence of sharp peaks in POA measurements inside the city, which magnitude is not captured by the model as explained in Sect. 5.1.

5   Analysis and interpretation of modeling results

The model performance in simulating various carbonaceous aerosol components is examined in Figs. 6 and 7. PMF analysis applied to AMS data allows separating total organic aerosols (TOA) into hydrocarbon-like organic aerosol (HOA, a POA surrogate), oxidized organic aerosol (OOA, a surrogate for SOA) and biomass burning organic aerosol (BBOA) for three locations in Mexico City (i.e. T0, T1, PTP). This specification allows more accurate evaluation of modeled TOA components as they have very different formation patterns: the modeled urban POA (SOA) can be compared directly to the observed HOA (OOA). The observed BBOA mass corresponds mainly to POA emitted by biomass burning activities. The SOA formed from BB precursors will likely be detected as OOA (Grieshop et al., 2009b) and this effect adds some uncertainty to our comparisons. However, as discussed in Aiken et al. (2009b) the impact of SOA from

BB precursors at T0 appears to be small during MILAGRO. Therefore, in the following sections we evaluate model results not only for TOA as it is usually done but also for individual contributions of POA and SOA. Table 4 summarizes the comparison results for SOA obtained for several sensitivity runs.

5.1 Total organic aerosol

The first panel of Fig. 6a, b, c compares the diurnal variation of observed and predicted near-surface total organic aerosols during MILAGRO. The observed TOA features high concentrations over the entire field campaign. Elevated TOA levels are found within the city basin with daily maximum concentrations ranging from 20 up to $70 \, \mu g \, m^{-3}$. The peak values observed on 11, 18 and 21 March are associated with biomass burning events as indicated by the difference between POA and POA-BBOA measurements shown on Fig. 6b and also reported by Aiken et al. (2009a). At this urban location, the model generally reproduces the diurnal variability found in TOA observations (correlation coefficient of 0.48). The comparison of observed and modeled average TOA diurnal profiles for March 2006 (Fig. 7) shows that the model correctly replicates the gradual increase in TOA concentrations during the day caused by both early morning primary emissions (13:00 UTC, i.e. 07:00 LT) and mid-day production of secondary species that starts around 18:00 UTC (12:00 LT). However, the modeled TOA only explains 55% of the observed organic material. This model underestimation is particularly large in the afternoon (17:00–23:00 UTC, i.e. 11:00–17:00 LT) suggesting a very inefficient production of secondary organic species in the model.

The observed surface TOA concentrations gradually decrease downwind of the city. A factor of 2 decrease could be noticed at the PTP elevated site, and a factor of 4 decrease at the T1 near-urban site (Fig. 7). At the T1 site, the highest TOA concentrations are associated with the downwind advection of pollutants from the city or the biomass burning events (e.g. 21 March). According to Doran et al. (2007), this site is much less affected by the Mexico City plume than expected, with the exception of 18, 19, 20, 24 and 27 March. The rest of the time regional background conditions pre-

vail. At this downwind location discrepancies between modeled and observed TOA are large both in terms of magnitude and temporal variability. Observed TOA concentrations are underestimated by a factor of 2–3 and the correlation with the measurements is reduced (R^2=0.28). While the observed TOA features a pronounced diurnal cycle with peak values at 12:00 UTC and 20:00 UTC, the modeled diurnal profile is rather uniform with large underprediction of the mid-day production of the aerosol due to the photochemistry. It should also be noticed that T1 is located at the northeastern border of the city that is growing continuously. This spatial expansion might not be reflected in the current emission inventory which could contribute to the model underprediction of aerosol concentrations.

The comparison with AMS data at the PTP site confirms model underestimation of TOA levels. Located on a hill only 10 km downwind of the city center, the PTP site is greatly influenced by urban activities. Because of its elevated topography (900 m above the city ground), TOA concentrations display however a very specific diurnal profile with a peak value occurring at 16:00 UTC, which is 3 h later than at T0 and T1. As explained in Fast et al. (2009) this sharp increase in concentrations at 18:00 UTC coincides with the growth of the PBL above the altitude of the station and the arrival of the city pollution.

This comparison clearly shows model difficulties in simulating TOA levels in this polluted region, difficulties that seem to increase with the distance from emission sources. Given that the model predicts reasonably well the concentrations of gas phase species, it is likely that the aerosol errors result either from an underestimation of POA emissions or an underestimation of SOA formation.

5.2 Primary organic aerosols

The second panel of Fig. 6a, b, c assesses model performance in simulating POA during March 2006 and the accuracy of primary emissions. At T0, CHIMERE successfully reproduces the observed POA diurnal variation (R^2=0.59) characterized by an early morning peak associated with traffic (Fig. 7). Predicted POA lies between measured

anthropogenic POA (crosses) and the measured total POA that accounts for both anthropogenic and biomass burning emissions. POA peak values are correctly simulated by the model most of the time, except as previously mentioned on three specific days (11, 18, 21 March) influenced by intense biomass burning activities. As shown in
⁵ Fig. 6a, for these days, the model tends to underestimate the observed peaks by a factor of 2 even though modeled POA takes into account biomass burning emissions. Possible reasons for this underprediction include: (I) the inaccurate representation of small burning activities (<1 km in size) within the city, which are currently unaccounted for in the emissions inventory (Yokelson et al., 2007); (II) the dilution of the smoke emis-
¹⁰ sions within $5 \times 5\,km^2$ model grid boxes which results in more spread BB plumes and smother gradients in POA concentrations associated with the fires. The comparison of diurnal profiles also shows the model tendency to overpredict nighttime concentrations. This pattern has already been seen for other primary species such as CO, and is most likely caused by a too shallow nighttime boundary layer over the basin. The agreement
¹⁵ is still reasonable at T1, although the model tends once again to underestimate by 15% the average morning POA peak concentrations as shown in Fig. 7. As previously mentioned, the emission inventory does not represent well the spatial expansion of the city at this location. In addition, the model spatial resolution ($5 \times 5\,km^2$) is too coarse to capture sharp spatial emission gradients associated with the presence of a major
²⁰ highway near T1.

At PTP, larger discrepancies between observed and modeled POA values are found. While POA average concentrations seem to be captured by the model with small positive bias, the predicted diurnal variability is inconsistent with observations. The predicted morning POA peak occurs 2–3 h earlier than observed. This time the shift most
²⁵ likely has a dynamic origin to it. As previously mentioned, the late arrival of pollutants over the elevated PTP site is associated with the growth of the PBL above 900 m (station's altitude). Although there is no evidence for the more rapid growth of the PBL height (see Fig. 5b) in the model, the unrealistic upslope winds (see Fig. 4) could be advecting city pollution more rapidly to PTP. In addition, as suggested by Fast et al. (2009),

the model horizontal resolution of 5 km is most likely insufficient in order to accurately resolve the topography of the PTP site. Therefore, the simulated peak height is several hundred meters lower than the actual height of this site, causing this site to stay all the time inside the polluted boundary layer. According to the difference between measured anthropogenic POA and total anthropogenic and BB POA it seems that the absolute contribution of biomass burning is reduced outside of the city ($<3\,\mu g\,m^{-3}$ at PTP and T1) compared to their influence within the city basin ($\sim 5\,\mu g\,m^{-3}$). This may be due to the closer location of most fires to T0 compared to T1. An alternative explanation is the influence of very small fires (from cooking, biofuel use, etc.) may be occurring within the city or that sources of partially oxidized aerosols such as meat cooking may be retrieved together with BBOA due to some similarities in the spectra of both POA sources (Mohr et al., 2009). However the results of Aiken et al. (2009a) suggest that this source is small since the BBOA concentration is very low during the days in which regional biomass burning is suppressed.

Diurnal POA profiles simulated by the CHIMERE model are very consistent with the results reported by Fast et al. (2009) for the WRF/Chem model suggesting that the treatment of primary aerosol emissions from both anthropogenic and biomass burning activities is correctly handled in this study. These results also show that primary emissions of organic aerosols do not have major biases and suggest that TOA underestimation is mainly caused by poor representation of secondary organic aerosols.

5.3 SOA formation from anthropogenic precursors

5.3.1 Reference run

SOA predictions from a reference model simulation (ANT-T) are first examined in order to quantify the amount of SOA that can be explained by the first-generation oxidation of anthropogenic precursors. According to Volkamer et al. (2006) SOA production from anthropogenic precursors accounted for over 95% of the calculated daytime SOA production within the city for their case study, during which there was very low back-

ground and regional influence (which is relatively unusual for Mexico City). Figure 7 presents the comparison of monthly mean diurnal profiles of predicted SOA and observed OOA at the 3 locations under study. The shape of the OOA diurnal profile features a strong enhancement in concentrations during the morning associated with an active photochemical production of SOA close to the emissions (i.e. T0, PTP). The diurnal variability is less pronounced at the peripheral T1 station and displays a more gradual increase of concentrations during the day. Similar to TOA concentrations, OOA surface levels gradually decrease downwind of the city with monthly average concentrations ranging from $7.5\,\mu g\,m^{-3}$ at T0 to $4.6\,\mu g\,m^{-3}$ at T1. Table 4 indicates that the reference run (i.e. ANT-T) severely underpredicts the observed OOA levels, typically by a factor of 5–10 for various stations. Figure 7 confirms that the predicted SOA values lie well below the observed ones and their associated variability range.

These results are certainly consistent in many ways with earlier studies performed in this region; however, an intriguing feature emerges from this comparison. As illustrated in Fig. 7, the predicted morning average SOA production rate of $4\mu g\,m^{-3}$ matches within a factor of 2 the intensity of the observed increase at the urban site in the early afternoon, although the discrepancy grows to a factor of 5–10 by 20:00 UTC (i.e. 14:00 LT). This similarity in the relative diurnal cycles when the background OOA is excluded explains the observed correlation with the OOA measurements. The comparison (see Supplement http://www.atmos-chem-phys-discuss.net/9/12207/2009/acpd-9-12207-2009-supplement.pdf, Fig. 3) also shows that the predicted SOA that was photochemicaly generated within the city tends to evaporate within the growing PBL during early afternoon, while the observed SOA stays elevated until late afternoon (22:00 UTC, i.e. 16:00 LT) despite the enhanced afternoon PBL mixing and lower OA concentrations available for the gas/aerosol partitioning. One possible reason for the increasing discrepancy later in the day is that as the aerosol ages the organic material tends to stay more permanently in the particle (despite dilution) which is not captured correctly in the model (i.e. the model evaporates half of the freshly produced SOA material). This is consistent with thermal denuder measurements at T0 which

showed that the measured OOA was significantly less volatile than typical model SOA, and that the more aged OOA (OOA-1) was less volatile than the fresher OOA (OOA-2) (Huffman et al., 2009; Dzepina et al., 2009). The sensitivity of model results to the gas/aerosol partitioning is discussed further below.

The large model underestimation is present throughout the day, about 6–8 $\mu g\,m^{-3}$ at T0 for example, suggesting that in addition to the local photochemical production, regional SOA levels might be underpredicted. Regional pollution is indeed advected into the city during the late afternoon under the influence of southerly winds that have the tendency to clean out pollutants generated during the day and bring cleaner regional concentrations. The fact that predicted SOA concentrations drop rapidly after the collapse of the PBL in the late afternoon to very low values ($<1\,\mu g\,m^{-3}$), and remain close to zero overnight is an additional indication that background levels are not well predicted and potentially also that the model SOA is too volatile. As expected, large discrepancies between modeled and observed SOA concentrations are observed at the two other sites.

5.3.2 Emissions of aromatics

Low SOA background levels are the result of an inefficient regional production of SOA which could be related to a number of uncertainties surrounding SOA formation. Anthropogenic emissions of SOA precursors certainly constitute one of them. The representation of VOC chemical composition, as well as their temporal and spatial variation is very crude in current inventories. The extensive dataset collected during MILAGRO campaign enables the evaluation of predicted VOC precursors. Figure 8 compares average diurnal profiles of predicted and observed mono-substituted (e.g. toluene, ethylbenzene) and poly-substituted (e.g. xylene, trimethylbenzene) aromatics at T0, which are the dominant anthropogenic SOA precursors in Mexico City according to traditional SOA models (Volkamer et al., 2006; Dzepina et al., 2009). Even qualitative comparison suggests that the model matches quite well with the observed concentrations both in terms of magnitude and temporal variation. A slight overestimation of the

morning peak is expected though as predicted aromatic surrogates include species that are not present in the measurements. As for other primary species, there is no indication of a systematic model bias for aromatic SOA precursors. This is consistent with the results of Fast et al. (2009), whom however point out that the concentrations of most other VOC types have significantly more problems than the aromatics. As OH is the oxidant controlling the chemistry of VOC precursor species, we have also verified that the model reasonably reproduces OH concentrations during this period (see Supplement http://www.atmos-chem-phys-discuss.net/9/12207/2009/acpd-9-12207-2009-supplement.pdf, Fig. 4). The model underestimates OH at night and overestimates the mid-day peak, but the overall average is well-captured.

5.3.3 Sensitivity to partitioning coefficients

Besides uncertainties in VOC emissions, the choice of parameters used in SOA equilibrium partitioning can make a large difference on predicted SOA levels in some cases (e.g. Simpson et al., 2007). In particular, determination of saturation vapor pressure and enthalpy of vaporization of semi-volatile aerosols remains highly uncertain (Kanakidou et al., 2005; Offenberg et al., 2006; Stainer et al, 2008; Faulhaber et al., 2009; Hallquist et al., 2009). Also, in the traditional lumped approach, chemically similar compounds are lumped into a single surrogate compound which is assigned a unique saturation pressure and vaporization enthalpy representative of the group. This surrogate compound undergoes only first generation oxidation which does not allow accurate representation of changes in volatility with increased degree of oxidation (i.e. decrease in volatility with aged material). These approximations can significantly affect the gas/aerosol partitioning and the amount of the predicted SOA. In addition, freshly absorbed organic species can further react inside the particle by oligomerization creating larger molecules with a lower vapor pressure that irreversibly stay inside the aerosol (e.g. Kroll and Seinfeld, 2005; Pun and Seigneur, 2007). If these processes are important and are not compensated by others such as fragmentation of molecules leading to more volatile species, the aerosol organic mass can increase as well as the aerosol

ability to absorb additional semi-volatile compounds.

Given the limited knowledge on these mechanisms, we do not attempt to include them in this study. To perform a first-order evaluation of their potential impact on predicted SOA concentrations, partitioning toward the particulate phase is artificially increased by lowering the saturation vapor pressure by two orders of magnitude (i.e. by a factor of 100 for all species). The ANT-EP sensitivity study should be seen therefore as an upper limit of the SOA production from traditional anthropogenic precursors when calculated with traditional model formulations (from the same initial amount of precursors as for ANT-T). Figure 7 shows the comparison between ANT-EP and the reference run for three stations under study. A near doubling of average predicted SOA concentrations can be noticed during the day. The early morning increase in the model now approaches the measured one at T0 and PTP soon after the start of the photochemistry and less so later on, leading to a better agreement with observations. The overall bias and root mean square error are decreased somewhat, but the model sill falls short of the observations. Despite these statistical improvements, the nighttime discrepancy is not reduced which is indicative of a missing formation process or precursor in the model.

5.4 Unexpectedly large contribution of biogenic precursors

5.4.1 Presence of biogenics

One of the SOA formation pathways that have not been explored so far in Mexico City is the production from biogenic precursors. Although SOA formation from anthropogenic pollution is significant in and downwind of urban areas, the global SOA burden is thought to have the largest contribution from biogenic sources, with a 50% contribution from isoprene (e.g. Tsigaridis and Kanakidou, 2007). The fraction of modern carbon within Mexico City (Marley et al., 2009; Aiken et al., 2009b) is higher than the estimates of the biomass burning contribution to OC (Stone et al., 2008; Aiken et al., 2009a, b), which leaves room for other sources such as biogenic SOA or urban sources

of modern carbon (Hildemann et al., 1994). The concentrations of biogenic precursors within the city are more than an order of magnitude lower than for the aromatics, and thus the formation of SOA from these species within the city is thought to be small (Volkamer et al., 2006; Dzepina et al., 2009). For example, Fortner et al. (2009) re-ported daily peak values of 1.7 ppb for isoprene and 1.2 ppb for monoterpenes at T0 (see Fig. 3 of Fortner et al., 2009) vs. 100 ppb for total aromatics. While isoprene can have both biogenic and anthropogenic origin, monoterpenes are clearly not produced by anthropogenic activities within the city, and are either advected from surrounding mountains or long-range transported from remote coastal areas.

Figure 1b shows the spatial distribution of isoprene emission fluxes estimated from the MEGAN model for March 2006 over Mexico and Central America. As expected, near the metropolitan area isoprene emissions are several orders of magnitude lower than those from aromatics (e.g. the flux of mono-substituted aromatics is estimated as 20 Tons/day within the city, not shown). However, much larger emissions of isoprene are found in the coastal regions, esp. southwest of Mexico City. Even though the lifetime of isoprene is relatively short ($\sim$1–2 h), SOA formed from these precursors has a much longer lifetime ($\sim$5–7 days) and can be long-range transported to Mexico City from the Southwest and the Gulf of Mexico under the influence of the regional winds contributing therefore to the SOA regional background levels. An order-of-magnitude estimate of the regional contribution of isoprene to SOA background concentrations is presented here to evaluate the potential importance of this source. Given a relatively low wind speed during this period, we assume that isoprene emitted within a 150 km radius around Mexico City can influence the regional SOA formation and reach the basin. Assuming a 2% SOA mass yield from isoprene, we estimate SOA regional production as approximately 20 Tons/day within the given perimeter. This estimate corresponds to an emission flux of SOA of approximately 290 μg/m^2/day, which results in a total production of $\sim$1.5 μg m^{-3} over 5 days period (assuming an average boundary layer dispersion of 1 km). This amount is of the same order of magnitude as SOA production from mono-substituted aromatics, estimated as 34 Tons/day in this same

region (assuming a 9.6% yield). These estimates suggest that biogenic SOA levels in the Mexico City region are far from negligible.

The influence of biogenic sources on predicted SOA levels in Mexico City by the CHIMERE model is quantified in Table 4. Compared to the reference simulation, the BIO-T run significantly reduces the model underprediction of SOA levels at all three stations. The model bias is reduced by more than 20% as well as the RMS error indicating an improved agreement with observations. A decrease in correlation coefficients is observed for the PTP site and could have a dynamic origin as already discussed for primary species. The increase in predicted SOA concentrations of $1–2\,\mu g\,m^{-3}$ is observed throughout the day as illustrated in Fig. 9. In particular, the comparison of SOA diurnal profiles between BIO-T and ANT-T runs shows that nighttime SOA levels are much better captured when biogenic sources are taken into account. SOA concentrations are reproduced within a factor of 3 at all sites, however predicted SOA diurnal profiles stay at the bottom edge of the observation variability interval.

Additional sensitivity runs (not shown here) have been carried out in order to determine whether biogenic SOA particles found within the basin have been locally produced on the hills surrounding Mexico City or long-range transported from the coastal region. Model results indicate that only a few percent of biogenic SOA has a local origin, the major fraction being produced upwind on the coastal areas and advected into the city. The largest contribution to biogenic SOA is from regional isoprene (>60%). Production from monoterpenes is smaller, which is consistent with the fact that emissions of monoterpenes are one to two orders of magnitude lower than those of isoprene in the model.

5.4.2 Role of anthropogenic emissions of isoprene

Although it seems very likely that regionally produced biogenic isoprene contributes significantly to SOA formation within the city, it should also be noted that isoprene concentrations are surprisingly elevated within the city throughout the day (1–2 ppb; see Fig. 8). The diurnal variability of isoprene concentrations has a strong anthropogenic

signature to it with peak concentrations occurring during traffic rush hours. The anthropogenic character of isoprene within the city is also confirmed by the comparison of observed concentrations with the results of two model runs at T0 (Fig. 8): the model sensitivity run BIO-ANT that accounts for anthropogenic emissions provides much better agreement with observations than the original BIO-T run. The anthropogenic isoprene is likely contributing to urban SOA formation, especially given its high reactivity. According to the results of the sensitivity run BIO-ANT, SOA formation from anthropogenic isoprene (with OH chemistry) is not negligible during MILAGRO: $0.20\,\mu g\,m^{-3}$ increase in the monthly mean SOA concentrations at T0.

5.4.3 Nighttime chemistry of isoprene

Finally, in addition to SOA formation from the reaction of isoprene with OH, we also investigate the importance of the oxidation of isoprene by NO_3 radicals. This reaction occurs only at night and consumes unreacted isoprene that has accumulated during the daytime. The recent study by Ng et al. (2008) estimated that the production of SOA from nighttime chemistry of isoprene is comparable to the production from aromatics on a global scale, and Brown et al. (2009) used aircraft observations of isoprene and NO_3 that this mechanism made a modest contribution to SOA formation over the New England region. Table 4 shows the effects of isoprene nighttime chemistry on the predicted total SOA in the vicinity of Mexico City. The average production of SOA is increased by approximately $0.15\,\mu g\,m^{-3}$ within Mexico City (run BIO-NT), leading to a slightly better agreement with the observations. However the effect of this mechanism is limited in comparison to the background SOA production from isoprene daytime chemistry, since the regions of high isoprene and high NO_3 radical are mostly disjoint.

5.4.4 Enhanced partitioning to the aerosol

Similar to anthropogenic precursors, biogenic SOA surrogates can be irreversibly partitioned to the aerosol phase as they undergo heterogeneous reactions inside the par-

ticles. Surratt et al. (2006) have identified the presence of oligomers among the SOA products of isoprene. If these processes are enhanced in the atmosphere compared to chamber studies, the SOA mass could be significantly increased. Because parameterizations for these reactions are currently unavailable, it is difficult to accurately quantify the fraction of the surrogate species that stays trapped inside the particle. Similar to the ANT-EP run, the partitioning to the aerosol phase was artificially increased by two orders of magnitude in order to provide a first-order estimate the upper limit for SOA concentrations that can be formed from biogenic sources present in the region. As expected, the BIO-EP run leads to an enhancement of SOA concentrations as a result of a greater partitioning of semivolatile species into the aerosol phase. The increase in concentrations is constant throughout the day ($\sim$2–3 μg m^{-3}) at all sites, as the BSOA is produced at the regional scale, upwind of the city. Even though a much better agreement is reached between modeled and observed SOA diurnal profiles (Fig. 9) with this run, correlation coefficients are decreased indicating higher spatio-temporal inconsistencies in the BSOA fields. In particular, the model bias has been significantly reduced in the early afternoon but not completely eliminated in the model predictions. The important conclusion from these results is that biogenic SOA formation is sensitive to the choice of partitioning parameters (which are currently highly uncertain). If chemical aging of semi-volatile gaseous precursors or oligomerization reactions within the particle could lower the vapor pressure species as much as assumed here, the predicted amount of the BSOA could increase by a factor of 2. This sensitivity to partitioning parameters has already been reported by Johnson et al. (2006) during the TORCH 2003 field study in the UK. In order to match the AMS-derived OOA concentrations, Johnson et al. (2006) had to increase all partitioning coefficients by a factor of 500 suggesting the occurrence of unaccounted chemical processes within the aerosol.

5.5 How large is the underpredicted SOA mass?

The interpretation of the comparison results for pollutant concentrations performed at the surface is largely dependent on the model ability to predict their vertical dispersion

within the boundary layer and the PBL depth itself. This dependence can be misleading, and drive our focus on solving discrepancies encountered during nighttime when errors are amplified due to the presence of shallow PBL. Here, we introduce another way of evaluating the predicted SOA levels based on comparisons of their column-integrated mass (within PBL) which is not influenced by the vertical dilution. Figure 10 shows the comparison of PBL-integrated SOA concentrations as observed at T0 and predicted by three model runs previously discussed (i.e. ANT-T, BIO-T and BIO-EP). The observed SOA column was calculated assuming a uniformly distributed SOA mass throughout the PBL (by multiplying the surface SOA concentrations by the PBL depth), while the modeled SOA concentrations were integrated within the predicted PBL. The comparison of the PBL-integrated SOA mass clearly shows that major discrepancies between the model and measurements occur during daytime (16:00–24:00 UTC, i.e. 10:00–18:00 LT) although the model underprediction of SOA surface concentrations by the reference run (ANT-T) appears to be constant when plotting surface concentrations (6–8 μg m^{-3}) throughout the day as previously shown. The model underprediction for the reference simulation (ANT-T) ranges from 2 mg/m^2 during the nighttime up to 23 mg/m^2 in the afternoon, which correspond roughly to an underprediction of the observed SOA mass over the MCMA region (assuming an area of 30×30 km^2) from 1.8 Tons at night and up to 20.7 Tons during the day. This underprediction is indeed similar to those reported by Volkamer et al. (2006); Kleinman et al. (2008), and Dzepina et al. (2009) when using traditional SOA models and using ratios of OOA to excess CO to remove the effect of dilution. Accounting for biogenic VOC precursors (BIO-T) contributes to reduce these discrepancies by half during the nighttime, however a large underestimation (up to 21 mg/m^2 or 18.9 Tons) persists during the day. This comparison once again highlights the limitations of the traditional SOA formation approach, and the need for more complex parameterizations for air quality models. Significant improvement in SOA predictions is obtained under the assumption of greatly enhanced partitioning of oxidized semi-volatile material with the aging of aerosol particles in the afternoon. As shown in Fig. 10, the BIO-NT run re-

Modeling organic aerosols during MILAGRO

A. Hodzic et al.

Full Screen / Esc

Printer-friendly Version

Interactive Discussion

produces fairly well the SOA levels at night and lies within the observation variability interval during the day. The model underprediction of the SOA mass is indeed reduced from ~20 Tons down to ~8 Tons as estimated in the early afternoon (20:00–21:00 UTC, i.e. 14:00–15:00 LT).

5.6 Discussion

Systematic evaluation of the predicted primary and secondary organic aerosols with highly time-resolved AMS data strongly suggests that anthropogenic emissions and biomass burning are not the only sources of SOA in Mexico City. Figure 11 shows the relative contributions of various emission sources to the predicted monthly mean SOA concentrations (from 4 to 31 March 2006) over the Mexico City region. The results presented are based on the integrated run (best-guess run BIO-NT) in which SOA is formed from all sources discussed above (i.e. anthropogenic, biogenic, nighttime chemistry as well as biomass burning). The % contribution is computed from monthly mean concentrations of source-tagged species.

In agreement with our previous analyses, model results indicate that anthropogenic SOA concentrations reach their highest values within the Mexico City basin close to the emission sources, and that they gradually decrease at the regional scale. The average SOA production from anthropogenic activities is estimated to be $3 \, \mu g \, m^{-3}$, and is comparable in magnitude to the predicted regional background ($\sim 2 \, \mu g \, m^{-3}$). The percentage contribution of various components to the total SOA amounts shows a strong spatial variability as illustrated in Fig. 11b–c. Within the Mexico City basin, predicted average contributions from anthropogenic and biogenic sources appear to be of the same order.

Although this result contrasts previous modeling studies, which reported that SOA formation within Mexico City was dominated by anthropogenic precursors (Volkamer et al., 2006; Kleinman et al., 2008), previous studies had not considered the advection into Mexico City of SOA formed on the regional scale. Note that our results provide an average estimate of this contribution during March 2006, which can vary from day-

Modeling organic aerosols during MILAGRO

A. Hodzic et al.

to-day based on meteorological conditions. For instance, this source was negligible during the case study of Volkamer et al. (2006) and Dzepina et al. (2009) due to the low backgrounds and wind speeds in that case which made SOA formation dominated by urban precursors. The presence of biogenic SOA is consistent with the high fraction of modern carbon in aerosol within the city reported by Marley et al. (2009) and Aiken et al. (2009b), which reaches 30–45% even during periods with low biomass burning. Similar to the fraction of modern carbon reported for the measurements which was higher at the T1 than T0 site (Marley et al., 2009), the relative importance of BSOA increases at the regional scale and represents more than 90% of the modeled SOA mass. One should keep in mind that these contributions are relative to the total predicted SOA amount. Clearly, if some sources are underestimated in the model the relative contribution of other species may appear unrealistically high.

Besides aromatic and biogenic precursors, there is reason to believe that semivolatile POA contributes greatly to the formation of SOA. A recent box-model study by Dzepina et al. (2009), suggested that these primary species could be responsible for more than 70% of the observed SOA within Mexico-City for a local-SOA dominated case study during the MCMA 2003 field project. The influence of this mechanism is evaluated in Hodzic et al. (2009) for the MILAGRO field project.

Finally, forest and agricultural burning also contribute to ambient SOA concentrations. Biomass burning emissions are included in all of our simulations as well as the SOA formation from fire-emitted VOCs. A sensitivity study (not shown here) has shown that their influence on SOA production is however limited (∼2%) in the model results and arises mainly in the hills surrounding Mexico City. The net effect of SOA formation from biomass burning on total BBOA mass is uncertain at present, different studies report results that vary between no net increase (Capes et al., 2008) and doubling of the primary BBOA (Yokelson et al., 2009). However Grieshop et al. (2009a) showed that SOA formation from traditional precursors significantly underpredicted the amount of SOA formed from some types of wood smoke in a smog chamber. Thus it is likely that our prediction of SOA formation from BB emissions is also biased low. Grieshop et

al. (2009a) suggest that the SOA formed from BB emissions is dominated by that from semivolatile and intermediate volatility species (SVOC + IVOC) which are not considered in current models, and the effect of this mechanism will be evaluated in the follow up study (Hodzic et al., 2009). From the point of view of the observations, the impact of SOA from BB emissions appears to have been limited at the T0 site during MILAGRO, mainly because the largest impact was observed in the early morning due to emissions in the evening which had not undergone photochemical processing (Aiken et al., 2009a). This finding is confirmed by the lack of variation of the OOA concentration between the high and low fire periods during MILAGRO (Aiken et al., 2009b).

6 Conclusions

This article uses an air quality model to investigate the processes controlling organic aerosols, with a particular focus on SOA formation, in the vicinity of Mexico City. The CHIMERE model results have been evaluated against aerosol mass spectrometry measurements at three ground sites in the framework of the 2006 MILAGRO field campaign. For the first time we were able to assess separately the model results for primary and secondary organic fractions during a month-long time period.

Because of complex meteorology associated with the Mexico City basin, the ability of the CHIMERE/MM5 model in simulating meteorological variables and dispersion of primary pollutants has been assessed (for the base case simulation) prior to the aerosol results. In addition to the base simulation, several sensitivity runs have been performed in order to address the question of the origin of SOA particles and the sensitivity to the choice of partitioning parameters. The following specific conclusions arise from the study:

(I) The model/measurement comparison shows absence of systematic bias in simulated meteorological variables that are responsible for pollutant dispersion and transport including wind speed and boundary layer height. A slightly underesti-

mated PBL overnight is suspected to lead to weak dispersion of primary-emitted species and their overestimation by the model.

(II) The comparison reveals an overall agreement between measured and simulated gas-species during the study period of March 2006.

(III) Observed concentrations of primary organic aerosols are reasonably reproduced by the model throughout the day indicating that there is no significant bias in aerosol primary emissions related to anthropogenic activities and biomass burning. Our modeling results on POA are consistent with previous studies (Fast et al., 2009) that used the same emissions and also considered POA as non-volatile.

(IV) Less than 15% of the observed SOA within the city can be explained by the traditional mechanism based on oxidation of anthropogenic precursors. The gap between modeled and observed concentrations strongly varies during the day. The model tends to capture within a factor of two the rapid photochemical production of SOA immediately after sunrise, however the discrepancy increases several fold during the day, and the observed nighttime SOA concentrations are severely underestimated (modeled SOA levels close to zero).

(V) Regional biogenic precursors (isoprene and monoterpenes) play an important role in regional SOA formation which is advected into Mexico City. Modeled SOA concentrations during nighttime are dominated by biogenics, with predicted BSOA levels close to $2\,\mu g\,m^{-3}$, reducing the model overall bias by 20% at all sites.

The presence of anthropogenic emissions of isoprene within the city and the SOA formation during nighttime from the oxidation of isoprene by NO_3, contribute an additional 15% increase in the total simulated SOA. However, accounting for both anthropogenic and biogenic SOA precursors as described by current models explains only 35% of the observed SOA within the city, showing the limitations of the traditional approach.

(VI) Concentrations of mono-substituted and poly-substituted aromatics are reasonably reproduced by the model which indicates that traditional anthropogenic SOA precursors are not underpredicted and are not responsible for the strong negative bias in modeled SOA. Similarly OH is reasonably reproduced by the model.

(VII) Gas/aerosol partitioning is poorly understood and constitutes a sensitive parameter for the prediction of SOA levels. Sensitivity runs indicate that a much better agreement with SOA observations can be achieved when vapor pressures of various organic compounds are artificially decreased by two orders of magnitude. This decrease may possibly happen if semi-volatile organic precursors undergo multiple generations of oxidations or if organic species oligomerize inside the particle leading to a less volatile mix of species. This artificially increase partitioning toward aerosol provides a first-order upper limit for the amount of SOA that can be formed using the traditional two-product mechanism from the initially available VOC precursors if polymerization processes were to be considered.

(VIII) The comparison of daily SOA profiles also pointed out the model inability to retain more permanently the freshly formed secondary organic aerosols inside the particulate phase during the afternoon hours. Although sensitivity runs with enhanced partitioning toward the aerosol phase provided more realistic daily average SOA concentrations, the comparison revealed the model tendency to excessively evaporate the freshly formed SOA particles during the early afternoon (characterized by higher PBL dilution and lower amount of primary organics available for the gas/aerosol partitioning). The model inability to simulate this persistent SOA fraction is suggestive of missing processes, such as oligomerization, likely to modify the nature of the partitioning species ad shift the equilibrium towards the particulate phase.

(IX) The comparison of the PBL column-integrated SOA mass at the T0 site allowed quantifying the missing SOA mass in the model in this region. We estimated that within the MCMA area the model underprediction ranges from 1 Ton at nighttime

Full Screen / Esc

Printer-friendly Version

Interactive Discussion

up to 20 Tons in the afternoon when considering the traditional SOA formation approach from both anthropogenic and biogenic VOC precursors. The assumed extreme enhanced partitioning toward the aerosol phase allowed reducing the model underprediction from a factor of 5($\sim$20 Tons) down to 30% ($\sim$8 Tons) during the day. This new way of evaluating the predicted SOA mass using the column-integrated concentration highlights the extent of the SOA mass underprediction in current models and the potential influence of this gap on the estimates of the aerosol direct radiative forcing in this region.

(X) The contribution of biomass burning to SOA production is very small in the model but it is likely underestimated. The effect of SOA formation from SVOC + IVOC emitted from BB sources will be evaluated in the follow-on study.

(XI) According to our modeling results, the relative contribution of biogenic SOA (modern carbon) to the predicted monthly mean SOA amount is in the range 40–65% at T0, and that ratio increases to 65–90% at the regional scale (T1) during MILA-GRO which is consistent with recent measurements of C^{14} (Marley et al., 2009; Aiken et al., 2009b) during low biomass burning periods.

Obtaining perfect agreement with the observed SOA values is extremely challenging, and it is beyond the objectives of this paper, because of large uncertainties involved at every step of the SOA modeling. We have identified one of the important missing processes in this region, but there are many more areas of uncertainties and directions for improvement to be considered. The results of the present work have an important impact on the way the future modeling studies in this region should be designed.

References

Aiken, A. C., Salcedo, D., Cubison, M. J., Huffman, J. A., DeCarlo, P. F., Ulbrich, I. M., Docherty, K. S., Sueper, D., Kimmel, J. R., Worsnop, D. R., Trimborn, A., Northway, M., Stone, E. A., Schauer, J. J., Volkamer, R., Fortner, E., de Foy, B., Wang, J., Laskin, A., Shutthanandan, V., Zheng, J., Zhang, R., Gaffney, J., Marley, N. A., Paredes-Miranda, G., Arnott, W. P., Molina, L. T., Sosa, G., and Jimenez, J. L.: Mexico City aerosol analysis during MILAGRO using high resolution aerosol mass spectrometry at the urban supersite (T0) - Part 1: Fine particle composition and organic source apportionment, Atmos. Chem. Phys. Discuss., 9, 8377–8427, 2009a,
http://www.atmos-chem-phys-discuss.net/9/8377/2009/.
Aiken, A. C., de Foy, B., Wiedinmyer, C., et al.: Mexico City Aerosol Analysis during MILA-GRO using High Resolution Aerosol Mass Spectrometry at the Urban Supersite (T0) – Part 2: Analysis of the Biomass Burning Contribution and the Modern Carbon Fraction, Atmos. Chem. Phys. Discuss., in preparation, 2009b.
Aiken, A. C., DeCarlo, P. F., Kroll, J. H., Worsnop, D. R., Huffman, J. A., Docherty, K., Ulbrich, I. M., Mohr, C., Kimmel, J. R., Sueper, D., Zhang, Q., Sun, Y., Trimborn, A., Northway, M., Ziemann, P. J., Canagaratna, M. R., Onasch, T. B., Alfarra, R., Prevot, A. S. H., Dommen, J., Duplissy, J., Metzger, A., Baltensperger, U., and Jimenez, J. L.: O/C and OM/OC Ratios of Primary, Secondary, and Ambient Organic Aerosols with High Resolution Time-of-Flight Aerosol, Mass. Spectrom. Environ. Sci. Technol., 42, 4478–4485, doi:10.1021/es703009q, 2008.
Bessagnet, B., Menut, L., Curci, G., Hodzic, A., et al.: Regional modeling of carbonaceous aerosol over Europe – Focus on Secondary Organic Aerosols, J. Atmos. Chem., submitted, 2009.
Bessagnet, B., Hodzic, A., Vautard, R., Beekmann, M., Cheinet, S., Honoré, C., Liousse, C., and Rouil, L.: Aerosol modeling with CHIMERE—preliminary evaluation at the continental scale, Atmos. Environ., 38, 2803–2817, 2004.
Brown, S. S., deGouw, J. A., Warneke, C., Ryerson, T. B., Dubé, W. P., Atlas, E., Weber, R. J., Peltier, R. E., Neuman, J. A., Roberts, J. M., Swanson, A., Flocke, F., McKeen, S.

Modeling organic aerosols during MILAGRO

A. Hodzic et al.

A., Brioude, J., Sommariva, R., Trainer, M., Fehsenfeld, F. C., and Ravishankara, A. R.: Nocturnal isoprene oxidation over the Northeast United States in summer and its impact on reactive nitrogen partitioning and secondary organic aerosol, Atmos. Chem. Phys., 9, 3027–3042, 2009,
http://www.atmos-chem-phys.net/9/3027/2009/.

CAM (Comision Ambiental Metropolitana): Inventario de Emisiones 2002 de la Zona Metropolitana del Valle de Mexico, Mexico, 2004.

Camredon, M., Aumont, B., Lee-Taylor, J., and Madronich, S.: The SOA/VOC/NO_x system: an explicit model of secondary organic aerosol formation, Atmos. Chem. Phys., 7, 5599–5610, 2007,
http://www.atmos-chem-phys.net/7/5599/2007/.

Canagaratna, M. R., Jayne, J. T., Jimenez, J. L., Allan, J. D., Alfarra, M. R, Zhang, Q., Onasch, T. B., Drewnick, F., Coe, H., Middlebrook, A., Delia, A., Williams, L. R., Trimborn, A. M., Northway, M. J., DeCarlo, P. F., Kolb, C. E., Davidovits, P., and Worsnop, D. R.: Chemical and Microphysical Characterization of Ambient Aerosols with the Aerodyne Aerosol Mass Spectrometer, Mass. Spectrom. Rev., 26, 185–222, 2007.

Capes, G., Johnson, B., McFiggans, G., Williams, P. I., Haywood, J., and Coe, H.: Aging of Biomass Burning Aerosols Over West Africa: Aircraft Measurements of Chemical Composition, Microphysical Properties, and Emission Ratios, J. Geophys. Res., 113, D00C15, doi:10.1029/2008JD009845, 2008.

Chung, S. H. and Seinfeld, J. H.: Global distribution and climate forcing of carbonaceous aerosols, J. Geophys. Res., 107(D19), 4407, doi:10.1029/2001JD001397, 2002.

Claeys, M., Graham, B., Vas, G., et al.: Formation of secondary organic aerosols through photooxidation of isoprene, Science, 303(5661), 1173–1176, 2004.

DeCarlo, P. F. , Kimmel, J. R., Trimborn, A., Northway, M. J., Jayne, J. T., Aiken, A. C., Gonin, M., Fuhrer, K., Horvath, T., Docherty, K., Worsnop, D. R., and Jimenez, J. L.: Field-Deployable, High-Resolution, Time-of-Flight Aerosol Mass Spectrometer, Anal. Chem., 78, 8281–8289, 2006.

DeCarlo, P. F., Dunlea, E. J., Kimmel, J. R., Aiken, A. C., Sueper, D., Crounse, J., Wennberg, P. O., Emmons, L., Shinozuka, Y., Clarke, A., Zhou, J., Tomlinson, J., Collins, D. R., Knapp, D., Weinheimer, A. J., Montzka, D. D., Campos, T., and Jimenez, J. L.: Fast airborne aerosol size and chemistry measurements above Mexico City and Central Mexico during the MILAGRO campaign, Atmos. Chem. Phys., 8, 4027–4048, 2008,

Modeling organic aerosols during MILAGRO

A. Hodzic et al.

http://www.atmos-chem-phys.net/8/4027/2008/.

de Foy, B., Varela, J. R., Molina, L. T., and Molina, M. J.: Rapid ventilation of the Mexico City basin and regional fate of the urban plume, Atmos. Chem. Phys., 6, 2321–2335, 2006, http://www.atmos-chem-phys.net/6/2321/2006/.

De Gouw, J. and Jimenez, J. L.: Organic Aerosols in the Earth's Atmosphere, Environ. Sci. Technol., in press, 2009.

Docherty, K. S., Stone, E. A., Ulbrich, I. M., DeCarlo, P. F., Snyder, D. C., Schauer, J. J., Peltier, R. E., Weber, R. J., Murphy, S. M., Seinfeld, J. H., Grover, B. D., Eatough, D. J., and Jimenez, J. L.: Apportionment of Primary and Secondary Organic Aerosols in Southern California during the 2005 Study of Organic Aerosols in Riverside (SOAR), Environ. Sci. Technol., 42, 7655–7662, doi:10.1021/es8008166, 2008.

Dockery, D. W., Schwartz, J., and Spengler J. D.: Air-pollution and daily mortality – association with particulates and acid aerosols, Environ. Res., 59, 362–373, 1992.

Donahue, N. M., Robinson, A. L., Stanier, C. O., and Pandis, S. N.: Coupled partitioning, dilution, and chemical aging of semivolatile organics, Environ. Sci. Technol., 40, 2635–2643, 2006.

Doran, J. C., Barnard, J. C., Arnott, W. P., Cary, R., Coulter, R., Fast, J. D., Kassianov, E. I., Kleinman, L., Laulainen, N. S., Martin, T., Paredes-Miranda, G., Pekour, M. S., Shaw, W. J., Smith, D. F., Springston, S. R., and Yu, X.-Y.: The T1–T2 study: evolution of aerosol properties downwind of Mexico City, Atmos. Chem. Phys., 7, 1585–1598, 2007, http://www.atmos-chem-phys.net/7/1585/2007/.

Doran, J. C. and Zhong, S: Thermally driven gap winds into the Mexico City basin, J. Appl. Meteorol., 39, 1330–1340, 2000.

Drewnick, F., Hings, S. S., DeCarlo, P. F., Jayne, J. T., Gonin, M., Fuhrer, K., Weimer, S., Jimenez, J. L., Demerjian, K. L., Borrmann, S., and Worsnop, D. R.: A new Time-of-Flight Aerosol Mass Spectrometer (ToF-AMS) – Instrument Description and First Field Deployment, Aerosol Sci. Tech., 39, 637–658, 2005.

Dudhia, J.: A nonhydrostatic version of the Penn State/NCAR mesoscale model: validation tests and simulation of an Atlantic cyclone and cold front, Mon. Weather Rev., 121, 1493–1513, 1993.

Dzepina, K., Volkamer, R. M., Madronich, S., Tulet, P., Ulbrich, I. M., Zhang, Q., Cappa, C. D., Ziemann, P. J., and Jimenez, J. L.: Evaluation of new secondary organic aerosol models for a case study in Mexico City, Atmos. Chem. Phys. Discuss., 9, 4417–4488, 2009,

Modeling organic aerosols during MILAGRO

A. Hodzic et al.

http://www.atmos-chem-phys-discuss.net/9/4417/2009/.

Edgerton, S. A., Bian, X., Doran, J. C., et al.:Particulate air pollution in Mexico City: A collaborative research project, J. Air Waste Manage., 49(10), 1221–1229, 1999.

Facchini, M. C., Mircea, M., Fuzzi, S., and Charlson, R. J.: Cloud albedo enhancement by surface-active organic solutes in growing droplets, Nature, 401, 257–259, 1999.

Fast, J. D., de Foy, B., Acevedo Rosas, F., Caetano, E., Carmichael, G., Emmons, L., McKenna, D., Mena, M., Skamarock, W., Tie, X., Coulter, R. L., Barnard, J. C., Wiedinmyer, C., and Madronich, S.: A meteorological overview of the MILAGRO field campaigns, Atmos. Chem. Phys., 7, 2233–2257, 2007,
http://www.atmos-chem-phys.net/7/2233/2007/.

Fast, J. D., Aiken, A. C., Allan, J., Alexander, L., Campos, T., Canagaratna, M. R., Chapman, E., DeCarlo, P. F., de Foy, B., Gaffney, J., de Gouw, J., Doran, J. C., Emmons, L., Hodzic, A., Herndon, S. C., Huey, G., Jayne, J. T., Jimenez, J. L., Kleinman, L., Kuster, W., Marley, N., Russell, L., Ochoa, C., Onasch, T. B., Pekour, M., Song, C., Ulbrich, I. M., Warneke, C., Welsh-Bon, D., Wiedinmyer, C., Worsnop, D. R., Yu, X.-Y., and Zaveri, R.: Evaluating simulated primary anthropogenic and biomass burning organic aerosols during MILAGRO: implications for assessing treatments of secondary organic aerosols, Atmos. Chem. Phys. Discuss., 9, 4805–4871, 2009,
http://www.atmos-chem-phys-discuss.net/9/4805/2009/.

Ginoux, P., Chin, M., Tegen, I., Prospero, J. M., Holben, B., Dubovik, O., and Lin, S.-J.: Sources and distributions of dust aerosols simulated with the GOCART model, J. Geophys. Res., 106, 20255–20273, 2001.

Griffin, R. J., Dabdub, D., and Seinfeld, J. H.: Secondary organic aerosol: I. Atmospheric chemical mechanism for production of molecular constituents, J. Geophys. Res., 107(D17), 4332, doi:10.1029/2001JD000541, 2002.

Guenther, A., Hewitt, C. N., Erickson, D., et al.: A global model of natural volatile organic compound emissions, J. Geophys. Res., 100(D5), 8873–8892, 1995.

Hallquist, M., Wenger, J. C., Baltensperger, U., Rudich, Y., Simpson, D., Claeys, M., Dommen, J., Donahue, N. M., George, C., Goldstein, A. H., Hamilton, J. F., Herrmann, H., Hoffmann, T., Iinuma, Y., Jang, M., Jenkin, M., Jimenez, J. L., Kiendler-Scharr, A., Maenhaut, W., McFiggans, G., Mentel, Th. F., Monod, A., Prévôt, A. S. H., Seinfeld, J. H., Surratt, J. D., Szmigielski, R., and Wildt, J.: The formation, properties and impact of secondary organic aerosol: current and emerging issues, Atmos. Chem. Phys. Discuss., 9, 3555–3762, 2009,

Modeling organic aerosols during MILAGRO

A. Hodzic et al.

http://www.atmos-chem-phys-discuss.net/9/3555/2009/.

Hamilton, J. F., Webb, P. J., Lewis, A. C., Hopkins, J. R., Smith, S., and Davy, P.: Partially oxidised organic components in urban aerosol using GCXGC-TOF/MS, Atmos. Chem. Phys., 4, 1279–1290, 2004,
http://www.atmos-chem-phys.net/4/1279/2004/.

Hauglustaine, D. A., Hourdin, F., Walters, S., Jourdain, L., Filiberti, M.-A., Larmarque, J.-F., and Holland, E. A.: Interactive chemistry in the Laboratoire de Météorologie Dynamique general circulationmodel : description and background tropospheric chemistry evaluation, J. Geophys. Res., 109, D04314, doi:10.1029/2003JD003957, 2004.

Henze, D. K. and Seinfeld, J. H.: Global secondary organic aerosol from isoprene oxidation, Geophys. Res. Lett., 33, L09812, doi:10.1029/2006GL025976, 2006.

Herndon, S. C., Onasch, T. B., Wood, E. C., Kroll, J. H., Canagaratna, M. R., Jayne, J. T., Zavala, M. A., Knighton, W. B., Mazzoleni, C., Dubey, M. K., Ulbrich, I. M., Jimenez, J. L., Seila, R., de Gouw, J. A., de Foy, B., Fast, J., Molina, L. T., Kolb, C. E., and Worsnop, D. R.: The Correlation of Secondary Organic Aerosol with Odd Oxygen in a Megacity Outflow, Geophys. Res. Lett., 35, L15804, doi:10.1029/2008GL034058, 2008.

Faulhaber, A., Klingbeil, B. M., Jimenez, J. L., Jayne, J. T., Worsnop, D. R., and Ziemann, P. J.: Characterization of a Thermodenuder-Particle Beam Mass Spectrometer System for the Study of Organic Aerosol Volatility and Composition, Atmos. Meas. Tech., 2, 15–31, 2009, http://www.atmos-meas-tech.net/2/15/2009/.

Fast, J. D. and Zhong, S.: Meteorological factors associated with inhomogeneous ozone concentrations within the Mexico City basin, J. Geophys. Res., 103, 18927–18946, 1998.

Fortner, E. C., Zheng, J., Zhang, R., Berk Knighton, W., Volkamer, R. M., Sheehy, P., olina, L., and André, M.: Measurements of Volatile Organic Compounds Using Proton Transfer Reaction Mass Spectrometry during the MILAGRO 2006 Campaign, Atmos. Chem. Phys., 9, 467–481, 2009,
http://www.atmos-chem-phys.net/9/467/2009/.

Grieshop, A. P., Logue, J. M., Donahue, N. M., and Robinson, A. L.: Laboratory investigation of photochemical oxidation of organic aerosol from wood fires 1: measurement and simulation of organic aerosol evolution, Atmos. Chem. Phys., 9, 1263–1277, 2009, http://www.atmos-chem-phys.net/9/1263/2009/.

Grieshop, A. P., Donahue, N. M., and Robinson, A. L.: Laboratory investigation of photochemical oxidation of organic aerosol from wood fires 2: analysis of aerosol mass spectrometer

Title Page

Abstract | Introduction

Conclusions | References

Tables | Figures

◄ | ►►

◄ | ►

Back | Close

Full Screen / Esc

Printer-friendly Version

Interactive Discussion

data, Atmos. Chem. Phys., 9, 2227–2240, 2009,
http://www.atmos-chem-phys.net/9/2227/2009/.

Guenther, A., Karl, T., Harley, P., Wiedinmyer, C., Palmer, P. I., and Geron, C.: Estimates of global terrestrial isoprene emissions using MEGAN (Model of Emissions of Gases and Aerosols from Nature), Atmos. Chem. Phys., 6, 3181–3210, 2006,
http://www.atmos-chem-phys.net/6/3181/2006/.

Hildemann, L. M., Klinedinst, D.B., Klouda, G. A., Currie, L. A. and Cass, G. R.: Sources of Urban Contemporary Carbon Aerosol, Environ. Sci. Technol., 28(9), 1565–1576, 1994.

Hodzic, A., Chepfer, H., Vautard, R., et al.: Comparison of aerosol chemistry transport model simulations with lidar and Sun photometer observations at a site near Paris, J. Geophys. Res., 109, D23201, doi:10.1029/2004JD004735, 2004.

Hodzic, A., Vautard, R., Bessagnet, B., et al.: Long-term urban aerosol simulation versus routine particulate matter observations, Atmos. Environ., 39, 5851–5864, 2005.

Hodzic, A., Vautard, R., Chazette, P., Menut, L., and Bessagnet, B.: Aerosol chemical and optical properties over the Paris area within ESQUIF project, Atmos. Chem. Phys., 6, 3257–3280, 2006,
http://www.atmos-chem-phys.net/6/3257/2006/.

Hodzic, A., Madronich, S., Bohn, B., Massie, S., Menut, L., and Wiedinmyer, C.: Wildfire particulate matter in Europe during summer 2003: meso-scale modeling of smoke emissions, transport and radiative effects, Atmos. Chem. Phys., 7, 4043–4064, 2007,
http://www.atmos-chem-phys.net/7/4043/2007/.

Hodzic, A., Madronich, S., Jimenez, J. L., et al.: Potential contribution of semi-volatile and intermediate volatility primary compounds to the formation of secondary organic aerosol (SOA) in the Mexico City plume, Atmos. Chem. Phys. Discuss., in preparation, 2009.

Huffman, J. A., Docherty, K. S., Aiken, A. C., Cubison, M. J., Ulbrich, I. M., DeCarlo, P. F., Sueper, D., Jayne, J. T., Worsnop, D. R., Ziemann, P. J., and Jimenez, J. L.: Chemically-resolved aerosol volatility measurements from two megacity field studies, Atmos. Chem. Phys. Discuss., 9, 2645–2697, 2009,
http://www.atmos-chem-phys-discuss.net/9/2645/2009/.

Iinuma, Y., Boge, O., Gnauk, T., and Herrmann, H.: Aerosol chamber study of the α-pinene/O$_3$ reaction: Influence of particle acidity on aerosol yields and products, Atmos. Environ., 38, 761–773, 2004.

IPCC 2007, Forster, P., Ramaswamy, V., Artaxo, P., Berntsen, T., Betts, R., Fahey, D. W.,

Modeling organic aerosols during MILAGRO

A. Hodzic et al.

Haywood, J., Lean, J., Lowe, D. C., Myhre, G., Nganga, J., Prinn, R., Raga, G., Schulz, M., and Van Dorland, R.: Changes in Atmospheric Constituents and in Radiative Forcing, in: Climate Change 2007: The Physical Science Basis. Contribution of Working Group I to the Fourth Assessment Report of the Intergovernmental Panel on Climate Change, edited by: Solomon, S., Qin, D., Manning, M., Chen, Z., Marquis, M., Averyt, K. B., Tignor, M., and Miller, H. J., Cambridge University Press, Cambridge, UK and NY, NY, USA, 2007.

Jang, M., Czoschke, N. M., Lee, S., and Kamens, R. M.: Heterogeneous atmospheric aerosol production by acid-catalyzed particle-phase reactions, Nature, 298, 814–817, 2002.

Johnson, D., Utembe, S. R., Jenkin, M. E., Derwent, R. G., Hayman, G. D., Alfarra, M. R., Coe, H., and McFiggans, G.: Simulating regional scale secondary organic aerosol formation during the TORCH 2003 campaign in the southern UK, Atmos. Chem. Phys., 6, 403–418, 2006,
http://www.atmos-chem-phys.net/6/403/2006/.

Kalberer, M., Paulsen, D., Sax, M., et al.: Identification of polymers as major components of atmospheric organic aerosols, Science, 303(5664), 1659–1662, 2004.

Kanakidou, M., Seinfeld, J. H., Pandis, S. N., Barnes, I., Dentener, F. J., Facchini, M. C., Van Dingenen, R., Ervens, B., Nenes, A., Nielsen, C. J., Swietlicki, E., Putaud, J. P., Balkanski, Y., Fuzzi, S., Horth, J., Moortgat, G. K., Winterhalter, R., Myhre, C. E. L., Tsigaridis, K., Vignati, E., Stephanou, E. G., and Wilson, J.: Organic aerosol and global climate modelling: a review, Atmos. Chem. Phys., 5, 1053–1123, 2005,
http://www.atmos-chem-phys.net/5/1053/2005/.

Kleindienst, T. E., Jaoui, M., Lewandowski, M., Offenberg, J. H., Lewis, C. W., Bhave, P. W., and Edney, E. O.: Estimates of the contributions of biogenic and anthropogenic hydrocarbons to secondary organic aerosol at a southeastern U.S. Location, Atmos. Environ., 41, 8288–8300, doi:10.1016/j.atmosenv.2007.06.045, 2007.

Kondo, Y., Miyazaki, Y., Takegawa, N., Miyakawa, T., Weber, R. J., Jimenez, J. L., Zhang, Q., and Worsnop, D. R.: Oxygenated and water-soluble organic aerosols in Tokyo, J. Geophys. Res.-Atmos., 112, D01203, doi:10.1029/2006JD007056, 2007.

Konovalov, I. B., Beekmann, M., Richter, A., and Burrows, J. P.: Inverse modelling of the spatial distribution of NOx emissions on a continental scale using satellite data, Atmos. Chem. Phys., 6, 1747–1770, 2006,
http://www.atmos-chem-phys.net/6/1747/2006/.

Kroll, J. H. and Seinfeld, J. H.: Representation of secondary organic aerosol laboratory cham-

ber data for the interpretation of mechanisms of particle growth, Environ. Sci. Technol., 39, 4159–4165, 2005.

Kroll, J. H., Ng, N. L., Murphy, S. M., Flagan, R. C., and Seinfeld, J. H.: Secondary organic aerosol formation from isoprene oxidation, Environ. Sci. Technol., 40, 1869–1877, 2006.

Lanz, V. A., Alfarra, M. R., Baltensperger, U., Buchmann, B., Hueglin, C., and Prévôt, A. S. H.: Source apportionment of submicron organic aerosols at an urban site by factor analytical modelling of aerosol mass spectra, Atmos. Chem. Phys., 7, 1503–1522, 2007, http://www.atmos-chem-phys.net/7/1503/2007/.

Lattuati, M.: Contribution à l'étude du bilan de l'ozone troposphérique à l'interface de l'Europe et de l'Atlantique Nord: Modélisation lagrangienne et mesures en altitude, Ph.D. Thesis, University Pierre et Marie Curie, Paris, France, 1997.

Liao, H., Henze, D. K., Seinfeld, J. H., Wu, S., and Mickley, L. J.: Biogenic secondary organic aerosol over the United States: Comparison of climatological simulations with observations, J. Geophys. Res., 112, D06201, doi:10.1029/2006JD007813, 2007.

Limbeck, A., Kulmala, M., and Puxbaum, H.: Secondary organic aerosol formation via heterogeneous reaction of gaseous isoprene on acidic particles, Geophys. Res. Lett., 30(19), 1996, doi:10.1029/2003GL017738, 2003.

Liu, Y., Chen, F., Warner, T., Swerdlin, S., Bowers, J., and Halvorson, S.: Improvements to surface flux computations in a non-local-mixing PBL scheme, and refinements on urban processes in the Noah land-surface model with the NCAR/ATEC real-time FDDA and forecast system, 20th Conference on Weather Analysis and Forecasting/16 Conference on Numerical Weather Prediction, Seattle, Washington, 2004.

Lei, W., de Foy, B., Zavala, M., Volkamer, R., and Molina, L. T.: Characterizing ozone production in the Mexico City Metropolitan Area: a case study using a chemical transport model, Atmos. Chem. Phys., 7, 1347–1366, 2007, http://www.atmos-chem-phys.net/7/1347/2007/.

Lim, H.-J., Carlton, A. C., and Turpin, B. J.: Isoprene forms secondary organic aerosol through cloud processing: model simulations, Environ. Sci. Technol., 39, 4441–4446, 2005.

Loosmore, G. and Cederwall, R.: Precipitation scavenging of atmospheric aerosols for emergency response applications: testing an updated model with new real-time data, Atmos. Env., 38, 993–1003, 2004.

Madronich, S., McKenzie, R. E., Bjorn, L. O., and Caldwell, M. M.: Changes in biologically active ultraviolet radiation reaching the earth's surface, J. Photochem. Photobiol., Biology,

Title Page

Abstract | Introduction

Conclusions | References

Tables | Figures

◀ | ▶

◀ | ▶

Back | Close

Full Screen / Esc

Printer-friendly Version

Interactive Discussion

46, 5–19, 1998.

Marley, N. A., Gaffney, J. S., Castro, T., Salcido, A., and Frederick, J.: Measurements of aerosol absorption and scattering in the Mexico City Metropolitan Area during the MILAGRO field campaign: a comparison of results from the T0 and T1 sites, Atmos. Chem. Phys., 9, 189–206, 2009,
http://www.atmos-chem-phys.net/9/189/2009/.

Martin-Reviejo M. and Wirtz K.: Is benzene a precursor for secondary organic aerosol?, Environ. Sci. Technol., 39, 1045–1054, 2005.

Marr, L. C., Dzepina, K., Jimenez, J. L., Reisen, F., Bethel, H. L., Arey, J., Gaffney, J. S., Marley, N. A., Molina, L. T., and Molina, M. J.: Sources and transformations of particle-bound polycyclic aromatic hydrocarbons in Mexico City, Atmos. Chem. Phys., 6, 1733–1745, 2006,
http://www.atmos-chem-phys.net/6/1733/2006/.

McMurry, P. H.: A review of atmospheric aerosol measurements, Atmos. Environ., 34, 1959–1999, 2000.

Moffet, R. C., de Foy, B., Molina, L. T., Molina, M. J., and Prather, K. A.: Measurement of ambient aerosols in northern Mexico City by single particle mass spectrometry, Atmos. Chem. Phys., 8, 4499–4516, 2008,
http://www.atmos-chem-phys.net/8/4499/2008/.

Mohr C., Huffman, J. A., Cubison, M. J., Aiken, A. C., et al.: Characterization of Primary Organic Aerosol Emissions from Meat Cooking, Trash Burning, and Motor Vehicles with High-Resolution Aerosol Mass Spectrometry and Comparison with Ambient and Chamber Observations, Environ. Sci. Technol., 43, 2443–2449, 2009.

Molina, L. T., Kolb, C. E., de Foy, B., Lamb, B. K., Brune, W. H., Jimenez, J. L., Ramos-Villegas, R., Sarmiento, J., Paramo-Figueroa, V. H., Cardenas, B., Gutierrez-Avedoy, V., and Molina, M. J.: Air quality in North America's most populous city overview of the MCMA-2003 campaign, Atmos. Chem. Phys., 7, 2447–2473, 2007,
http://www.atmos-chem-phys.net/7/2447/2007/.

Molina, L. T., Madronich, S., Gaffney, J. S., and Singh, H. B.: Overview of MILAGRO/INTEX-B Campaign, IGACtivities Newsletter, Issue 38, 2–15, 2008.

Müller, J.-F., Stavrakou, T., Wallens, S., De Smedt, I., Van Roozendael, M., Potosnak, M. J., Rinne, J., Munger, B., Goldstein, A., and Guenther, A. B.: Global isoprene emissions estimated using MEGAN, ECMWF analyses and a detailed canopy environment model, Atmos.

Modeling organic aerosols during MILAGRO

A. Hodzic et al.

Chem. Phys., 8, 1329–1341, 2008,
http://www.atmos-chem-phys.net/8/1329/2008/.

Murphy, D. M.: Something in the air, Science, 307, 1888–1890, 2005.

Murphy, D. M., Cziczo, D. J., Froyd, K. D., Hudson, P. K., Matthew, B. M., Middlebrook, A. M., Peltier, R. E., Sullivan, A., Thomson, D. S., and Weber, R. J.: Single-particle mass spectrometry of tropospheric aerosol particles, J. Geophys. Res., 111, D23S32, doi:10.1029/2006JD007340, 2006.

Nemitz, E., Jimenez, J. L., Huffman, J. A., Canagaratna, M. R., Worsnop, D. R. and Guenther, A. B.: An eddy-covariance system for the measurement of surface/atmosphere exchange fluxes of submicron aerosol chemical species – first application above an urban area, Aerosol Sci. Tech., 42, 636–657, 2008.

Nenes, A., Pilinis, C., and Pandis, S.: ISORROPIA: A new thermodynamic model for inorganic multicomponent atmospheric aerosols, Aquat. Geochem., 4, 123–152, 1998.

Ng, N. L., Kwan, A. J., Surratt, J. D., Chan, A. W. H., Chhabra, P. S., Sorooshian, A., Pye, H. O. T., Crounse, J. D., Wennberg, P. O., Flagan, R. C., and Seinfeld, J. H.: Secondary organic aerosol (SOA) formation from reaction of isoprene with nitrate radicals (NO_3), Atmos. Chem. Phys., 8, 4117–4140, 2008,
http://www.atmos-chem-phys.net/8/4117/2008/.

Odum, J. R., Hoffmann, T., Bowman, F., Collins, D., Flagan, R. C., and Seinfeld, J. H.: Gas/particle partitioning and secondary organic aerosol yields, Environ. Sci. Technol., 30, 2584–2585, 1996.

Paatero, P. and Tapper, U.: Positive matrix factorization: A non-negative factor model with optimal utilization of error estimates of data values, Environmetrics, 5, 111–126, 1994.

Pankow, J. F.: An absorption model of gas/particle partitioning of organic compounds in the atmosphere, Atmos. Environ., 28, 185–188, 1994.

Paredes-Miranda, G., Arnott, W. P., Jimenez, J. L., Aiken, A. C., Gaffney, J. S., and Marley, N. A.: Primary and secondary contributions to aerosol light scattering and absorption in Mexico City during the MILAGRO 2006 campaign, Atmos. Chem. Phys. Discuss., 8, 16951–16979, 2008,
http://www.atmos-chem-phys-discuss.net/8/16951/2008/.

Prenni, A. J., Petters, M. D., Kreidenweis, S. M., DeMott, P. J., and Ziemann, P. J.: Cloud droplet activation of secondary organic aerosol, J. Geophys. Res., 112, D10223, doi:10.1029/2006JD007963, 2007.

Modeling organic aerosols during MILAGRO

A. Hodzic et al.

Title Page

Abstract | Introduction

Conclusions | References

Tables | Figures

◄ | ►►

◄ | ►

Back | Close

Full Screen / Esc

Printer-friendly Version

Interactive Discussion

Pun, B., Wu, S., Seigneur, C., Seinfeld, J., Griffin, R., and Pandis, A.: Uncertainties in modeling secondary organic aerosols: Three-dimensional modeling studies in Nashville/western Tennessee, Environ. Sci. Technol., 37, 3647–3661, 2003.

Pun, B.: Modeling secondary organic aerosol formation via multiphase partitioning with molecular data, Environ. Sci. Technol., 40, 4722–4731, 2006.

Pun, B.: Hydrophilic/Hydrophobic organic aerosol partition model – User' Manual, INERIS, Doc. Nb. CP198-05-01, July 2005

Pun, B. K. and Seigneur, C.: Investigative modeling of new pathways for secondary organic aerosol formation, Atmos. Chem. Phys., 7, 2199–2216, 2007,
http://www.atmos-chem-phys.net/7/2199/2007/.

Querol, X., Pey, J., Minguillón, M. C., Pérez, N., Alastuey, A., Viana, M., Moreno, T., Bernabé, R. M., Blanco, S., Cárdenas, B., Vega, E., Sosa, G., Escalona, S., Ruiz, H., and Artíñano, B.: PM speciation and sources in Mexico during the MILAGRO-2006 Campaign, Atmos. Chem. Phys., 8, 111–128, 2008,
http://www.atmos-chem-phys.net/8/111/2008/.

Robinson, A. L., Donahue, N. M., Shrivastava, M. K., Weitkamp, E. A., Sage, A. M., Grieshop, A. P., Lane, T. E., Pandis, S. N., Pierce, J. R.: Rethinking organic aerosols: Semivolatile emissions and photochemical aging, Science, 315, 1259–1262, 2007.

Salcedo, D., Onasch, T. B., Dzepina, K., Canagaratna, M. R., Zhang, Q., Huffman, J. A., De-Carlo, P. F., Jayne, J. T., Mortimer, P., Worsnop, D. R., Kolb, C. E., Johnson, K. S., Zuberi, B., Marr, L. C., Volkamer, R., Molina, L. T., Molina, M. J., Cardenas, B., Bernabé, R. M., Márquez, C., Gaffney, J. S., Marley, N. A., Laskin, A., Shutthanandan, V., Xie, Y., Brune, W., Lesher, R., Shirley, T., and Jimenez, J. L.: Characterization of ambient aerosols in Mexico City during the MCMA-2003 campaign with Aerosol Mass Spectrometry: results from the CENICA Supersite, Atmos. Chem. Phys., 6, 925–946, 2006,
http://www.atmos-chem-phys.net/6/925/2006/.

Shaw, W. J., Pekour, M. S., Coulter, R. L., Martin, T. J., and Walters, J. T.: The daytime mixing layer observed by radiosonde, profiler, and lidar during MILAGRO, Atmos. Chem. Phys. Discuss., 7, 15025–15065, 2007,
http://www.atmos-chem-phys-discuss.net/7/15025/2007/.

Simpson, D., Yttri, K. E., Klimont, Z., Kupiainen, K., Caseiro, A., Gelencsér, A., Pio, C., Puxbaum, H., and Legrand, M.: Modeling carbonaceous aerosol over Europe: Analysis of the CARBOSOL and EMEP EC/OC campaigns, J. Geophys. Res., 112, D23S14,

doi:10.1029/2006JD008158, 2007.

Simpson, D., Winiwarter, W., Borjesson, G., et al.: Inventorying emissions from nature in Europe, J. Geophys. Res., 104(D7), 8113–8152, 1999.

Song, C., Zaveri, R. A., Alexander, M. L., Thornton, J. A., Madronich, S., Ortega, J. V., Zelenyuk, A. N., Yu, X. Y., Laskin, A., and Maughan, A. D.: Effect of Hydrophobic Primary Organic Aerosols on Secondary Organic Aerosol Formation from Ozonolysis of α-Pinene, Geophys. Res. Lett., 34(20), L20803, doi:10.1029/2007GL030720, 2007.

Stephens, S., Madronich, S., Wu, F., Olson, J. B., Ramos, R., Retama, A., and Muñoz, R.: Weekly patterns of Mxico City's surface concentrations of CO, NO_x, PM_{10} and O_3 during 1986-2007, Atmos. Chem. Phys., 8, 5313–5325, 2008,
http://www.atmos-chem-phys.net/8/5313/2008/.

Stern, R., Builtjes, P., Schaap, M., Timmermans, R., Vautard, R., Hodzic, A., Memmesheimer, M., Feldmann, H., Renner, R., Wolke, R., and Kerschbaumer, A.: PA model inter-comparison study focussing on episodes with elevated PM_{10} concentrations, Atmos. Environ., 42(19), 4567–4588, 2008.

Stroud, C. A., Roberts, J. M., Williams, E. J., et al.: Nighttime isoprene trends at an urban forested site during the 1999 Southern Oxidant Study, J. Geophys. Res., 107(D16), 4291, doi:10.1029/2001JD000959, 2002.

Surratt, J. D., Murphy, S. M., Kroll, J. H., et al.: Chemical composition of secondary organic aerosol formed from the photooxidation of isoprene, J. Phys. Chem., 110, 9665–9690, 2006.

Tao, F., Gonzalez-Flecha, B., and Kobzik, L.: Reactive oxygen species in pulmonary inflammation by ambient particles, Free Rad. B., 35, 327–340, 2003.

Troen, I. and Mahrt, L.: A simple-model of the atmospheric boundary layer - Sensitivity to surface evaporation, Bound. Lay. Meteorol., 37(1–2), 129–148, 1986.

Tsigaridis, K. and Kanakidou, M.: Secondary organic aerosol importance in the future atmosphere, Atmos. Environ., 41, 4682–4692, 2007.

Tsyro, S.: First estimates of the effect of aerosol dynamics in the calculation of PM_{10} and $PM_{2.5}$, EMEP report, 2002.

Turpin, B. J., Saxena, P., and Andrews, E.: Measuring and simulating particulate organics in the atmosphere: problems and prospects, Atmos. Environ., 34(18), 2983–3013, 2000.

Ulbrich, I. M., Canagaratna, M. R., Zhang, Q., Worsnop, D. R., and Jimenez, J. L.: Interpretation of organic components from Positive Matrix Factorization of aerosol mass spectrometric data, Atmos. Chem. Phys., 9, 2891–2918, 2009,

Modeling organic aerosols during MILAGRO

A. Hodzic et al.

Title Page

Abstract | Introduction

Conclusions | References

Tables | Figures

◄◄ | ►►

◄ | ►

Back | Close

Full Screen / Esc

Printer-friendly Version

Interactive Discussion

http://www.atmos-chem-phys.net/9/2891/2009/.

Varutbangkul, V., Brechtel, F. J., Bahreini, R., Ng, N. L., Keywood, M. D., Kroll, J. H., Flagan, R. C., Seinfeld, J. H., Lee, A., and Goldstein, A. H.: Hygroscopicity of secondary organic aerosols formed by oxidation of cycloalkenes, monoterpenes, sesquiterpenes, and related compounds, Atmos. Chem. Phys., 6, 2367–2388, 2006, http://www.atmos-chem-phys.net/6/2367/2006/.

Vay, S. A., Tyler, S. C., Choi, Y., Blake, D. R., Blake, N. J., Sachse, G. W., Diskin, G. S., and Singh, H. B.: Sources and transport of $\delta^{14}C$ on CO_2 within the Mexico City Basin and vicinity, Atmos. Chem. Phys. Discuss., 9, 7213–7237, 2009, http://www.atmos-chem-phys-discuss.net/9/7213/2009/.

Velasco, E., Lamb, B., Westberg, H., Allwine, E., Sosa, G., Arriaga-Colina, J. L., Jobson, B. T., Alexander, M. L., Prazeller, P., Knighton, W. B., Rogers, T. M., Grutter, M., Herndon, S. C., Kolb, C. E., Zavala, M., de Foy, B., Volkamer, R., Molina, L. T., and Molina, M. J.: Distribution, magnitudes, reactivities, ratios and diurnal patterns of volatile organic compounds in the Valley of Mexico during the MCMA 2002 & 2003 field campaigns, Atmos. Chem. Phys., 7, 329–353, 2007, http://www.atmos-chem-phys.net/7/329/2007/.

Volkamer, R., Jimenez, J. L., San Martini, F., Dzepina, K., Zhang, Q., Salcedo, D., Molina, L. T., Worsnop, D. R., and Molina, M. J.: Secondary organic aerosol formation from anthropogenic air pollution: Rapid and higher than expected, Geophys. Res. Lett., 33, L17811, doi:10.1029/2006GL026899, 2006.

Volkamer, R., San Martini, F., Molina, L. T., Salcedo, D., Jimenez, J. L., and Molina, M. J: A Missing Sink for Gas-Phase Glyoxal in Mexico City: Formation of Secondary Organic Aerosol, Geophys. Res. Lett. 34, L19807, doi:10.1029/2007GL030752, 2007.

Volkamer, R., Ziemann, P. J., and Molina, M. J.: Secondary Organic Aerosol Formation from Acetylene (C_2H_2): seed effect on SOA yields due to organic photochemistry in the aerosol aqueous phase, Atmos. Chem. Phys., 9, 1907–1928, 2009, http://www.atmos-chem-phys.net/9/1907/2009/.

Warneck, P.: In-cloud chemistry opens pathway to the formation of oxalic acid in the marine atmosphere, Atmos. Environ., 37, 2423–2427, 2003.

Warneke C., de Gouw, J. A., Del Negro, L., Brioude, J., McKeen, S., Stark, H., Kuster, W. C., Goldan, P. D., Trainer, M., Fehsenfeld, F. C., Wiedinmyer, C., Guenther, A. B., Hansel, A., Wisthaler, A., Atlas, E., Huey, L. G., and Case Hanks, A. T.: Determination of Biogenic

Title Page

Abstract | Introduction

Conclusions | References

Tables | Figures

|◄ | ►|

◄ | ►

Back | Close

Full Screen / Esc

Printer-friendly Version

Interactive Discussion

Emissions in the Eastern United States and Texas and Comparison with Biogenic Emission Inventories, J. Geophys. Res., submitted, 2009.

Wesely, M. L.: Parameterization of surface resistance of gaseous dry deposition in regional-scale numerical models, Atmos. Environ., 23, 1293–1304, 1989.

5   Williams, B. J., Goldstein, A. H., Millet, D. B., Holzinger, R., Kreisberg, N. M., Hering, S. V., Allan, J. D., Worsnop, D. R., Jimenez, J. L., and White, A. B.: Chemical Speciation of Organic Aerosol during ICARTT 2004: Results from In-Situ Measurements, J. Geophys. Res.-Atmos., 112, D10S26, doi:10.1029/2006JD007601, 2007.

West, J. J., Zavala, M. A., Molina, L. T., Molina, M. J., San Martini, F., McRae, G. J., Sosa-

10   Iglesias, G., and Arriaga-Colina: J. L.: Modeling ozone photochemistry and evaluation of hydrocarbon emissions in the Mexico City metropolitan area, J. Geophys. Res., 109, D19312, doi:10.1029/2004JD004614, 2004.

Yttri, K. E., Aas, W., Bjerke, A., Cape, J. N., Cavalli, F., Ceburnis, D., Dye, C., Emblico, L., Facchini, M. C., Forster, C., Hanssen, J. E., Hansson, H. C., Jennings, S. G., Maenhaut,

15   W., Putaud, J. P., and Tørseth, K.: Elemental and organic carbon in PM_{10}: a one year measurement campaign within the European Monitoring and Evaluation Programme EMEP, Atmos. Chem. Phys., 7, 5711–5725, 2007,
http://www.atmos-chem-phys.net/7/5711/2007/.

Yokelson, R., Crounse, J. D., DeCarlo, P. F., Karl, T., Urbanski, S., Atlas, E., Campos, T.,

20   Shinozuka, Y., Kapustin, V., Clarke, A. D., Weinheimer, A., Knapp, D. J., Montzka, D. D., Holloway, J., Weibring, P., Flocke, F., Zheng, W., Toohey, D., Wennberg, P. O., Wiedinmyer, C., Mauldin, L., Fried, A., Richter, D., Walega, J., Jimenez, J. L., Adachi, K., Buseck, P. R., Hall, S. R., and Shetter, R.: Emissions from biomass burning in the Yucatan, Atmos. Chem. Phys. Discuss., 9, 767–835, 2009,

25   http://www.atmos-chem-phys-discuss.net/9/767/2009/.

Zaveri, R. A., Song, C., Alexander, L., et al.: Unraveling Contributions of Urban, Biomass Burning and Secondary Organic Aerosols Near Mexico City During MILAGRO 2006, Eos Trans. AGU, 89(53), Fall Meet. Suppl., Abstract A31B-0085, 2008.

Zhang, Y., Liu, P., Queen, A., Misenis, C., Pun, B., Seigneur, C., and Wu, S. Y.: A comprehen-

30   sive performance evaluation of MM5-CMAQ for the summer 1999 Southern Oxidants Study episode, Part II: gas and aerosol predictions, Atmos. Environ., 40, 4825-4838, 2006.

Zhang, Q., Alfarra, M. R., Worsnop, D. R., Allan, J. D., Coe, H., Canagaratna, M. R., and Jimenez, J. L.: Deconvolution and quantification of hydrocarbon-like and oxygenated or-

Title Page

Abstract | Introduction

Conclusions | References

Tables | Figures

◄ | ►

◄ | ►

Back | Close

Full Screen / Esc

Printer-friendly Version

Interactive Discussion

ganic aerosols based on aerosol mass spectrometry, Environ. Sci. Technol., 39, 4938–4952, 2005a.

Zhang, Q., Worsnop, D. R., Canagaratna, M. R., and Jimenez, J. L.: Hydrocarbon-like and oxygenated organic aerosols in Pittsburgh: insights into sources and processes of organic aerosols, Atmos. Chem. Phys., 5, 3289–3311, 2005, http://www.atmos-chem-phys.net/5/3289/2005/.

Zhang, Q., Canagaratna, M. R., Jayne, J. T., Worsnop, D. R., and Jimenez, J. L.: Time and Size-Resolved Chemical Composition of Submicron Particles in Pittsburgh – Implications for Aerosol Sources and Processes, J. Geophys. Res.-Atmos., 110, D07S09, doi:10.1029/2004JD004649, 2005c.

Zhang, Q., Jimenez, J. L., Canagaratna, M. R., et al.: Ubiquity and dominance of oxygenated species in organic aerosols in anthropogenically-influenced Northern Hemisphere midlatitudes, Geophys. Res. Lett., 34, L13801, doi:10.1029/2007GL029979, 2007.

Zheng, J., Zhang, R., Fortner, E. C., Volkamer, R. M., Molina, L., Aiken, A. C., Jimenez, J. L., Gaeggeler, K., Dommen, J., Dusanter, S., Stevens, P. S., and Tie, X.: Measurements of HNO3 and N2O5 using ion drift-chemical ionization mass spectrometry during the MILAGRO/MCMA-2006 campaign, Atmos. Chem. Phys., 8, 6823–6838, 2008, http://www.atmos-chem-phys.net/8/6823/2008/.

Zhong, S. Y. and Fast, J.: An evaluation of the MM5, RAMS, and Meso-Eta models at sub-kilometer resolution using VTMX field campaign data in the Salt Lake Valley, Mon. Weather Rev., 131, 1301–1322, 2003.

Modeling organic aerosols during MILAGRO

A. Hodzic et al.

Title Page

Abstract	Introduction
Conclusions	References
Tables	Figures

◄◄   ►►

◄   ►

Back   Close

Full Screen / Esc

Printer-friendly Version

Interactive Discussion

Table 1. Gas-phase chemical mechanism for SOA formation as used in the CHIMERE model.

VOC Precursors	Oxidation Reactions	Kinetics (cm^3 molec^{-1} s^{-1})
Toluene	TOL[a, b]+OH→0.005 AnA1D+0.084 AnBmP+0.013 AnBlP	1.81×10^{-12}exp(355/T)
Tri-methyl-benzene	TMB[a, b]+OH→0.005 AnA1D+0.088 AnBmP+0.006 AnBlP	9.80×10^{-9}/T
Higher alkanes	ALK[c]+OH→0.07 AnBmP	1.36×10^{-12}exp(190/T)(300/T)$^{-2}$
α−pinene and sabinene	APIN[a]+OH→0.57 BiA1D	1.21×10^{-11}exp(444/T)
	APIN[a]+NO$_3$→0.80 BiBmP	1.19×10^{-12}exp(490/T)
	APIN[a]+O$_3$→0.39 BiA1D	1.01×10^{-15}exp(-732/T)
β−pinene and δ^3-carene	BPIN[a]+OH→0.21 BiA1D	2.38×10^{-11}exp(357/T)
	BPIN[a]+NO$_3$→0.80 BiBmP	2.51×10^{-12}
	BPIN[a]+O$_3$→0.26 BiA1D	1.50×10^{-17}
Limonene	LIM[a]+OH→0.455 BiA1D	1.71×10^{-10}
	LIM[a]+O$_3$→0.19 BiA1D	2.0×10^{-16}
Octimene and mycene	TPO[a]+OH→0.775 BiA1D	5.1×10^{-16}/T
	TPO[a]+NO$_3$→0.775 BiA1D	4.3×10^{-9}/T
	TPO[a]+O$_3$→0.555 BiA1D	7.5×10^{-14}/T
Isoprene	ISO[d]+OH→0.232 ISO1+0.0288 ISO2	2.55×10^{-11}exp(410/T)
	ISO[e]+NO$_3$→0.089 ISO3+0.203 ISO4	7.0×10^{-13}

[a] Simplified mechanism based on Pun et al. (2005, 2006); in this study all hydrophilic oxidation products were grouped into a single surrogate compound (AnA1D for anthropogenics and BiA1D for biogenics) in order to increase the computational efficiency. The stoichiometric coefficient for this product was derived from the sum of the stoichiometric coefficients of individual hydrophilic oxidation products used in the base model presented by Pun et al. (2005, 2006). According to several studies (e.g. Pun et al., 2003, 2006) based on laboratory experiments, most SOA products present in the particulate phase are hydrophobic (Pun et al., 2003 reported >80% of hydrophobic SOA in their simulation in the southern US). Therefore, grouping hydrophilic oxidation products into a single hydrophilic compound (AnA1D for anthropogenic and BiA1D for biogenic species) with moderate saturation vapour pressure characteristics is a reasonable assumption. The following molecular weight (g/mol) and enthalpy of vaporization (kJ/mol) were considered for SOA surrogates: AnA1D (168 g/mol; 88 kJ/mol), AnBmP (152 g/mol; 88 kJ/mol), AnBlP (167 g/mol; 88 kJ/mol), BiA1D (170 g/mol; 88 kJ/mol), BiBmP (236 g/mol; 175 kJ/mol).

[b] Emissions of anthropogenic VOCs are grouped into classes of precursors: all mono-substituted single-ring aromatic compounds such as toluene and ethylbenzene are combined as high SOA yield aromatic precursors with toluene (TOL) as representative precursor. All poly-substituted single-ring aromatic compounds such as xylene and trimethylbenzene are combined as low SOA yield aromatic precursors with trimethylbenzene (TMB) as representative precursor (Pun et al., 2006).

[c] Ssimilar to Bessagnet et al. (2009).

[d] Henze and Seinfeld (2006) formulation under low-NOx conditions.

[e] Nighttime chemistry of isoprene following Ng et al. (2008).

Table 2. Proprieties of hydrophobic organic aerosols in CHIMERE.

Condensable Species	Saturation vapor pressure (Pa)[a]	Partition coefficient ($m^3/\mu g$)	Saturation concentration ($\mu g/m^3$)	Vaporization enthalpy (kJ/mol)
AnBIP	2.67×10^{-7}	/	1.8×10^{-2}	88
AnBmP	4.0×10^{-4}	/	24.54	88
BiBIP	8.0×10^{-8}	/	9.62×10^{-3}	175
BiBmP	4.0×10^{-5}	/	3.81	175
ISO1	/	8.62×10^{-3}	116	88
ISO2	/	1.62	0.62	88
ISO3	/	1.82×10^{-4}	5495	88
ISO4	/	4.6×10^{-5}	21 739	88

[a] the partitioning parameters are given at 298 K for AnBIP, AnBmP, BiBIP, BiBmP, and 295 K for isoprene derived species.

Table 3. Description of the CHIMERE model simulations carried out in this study.

Name of the experiment	Description of the model run
ANT-T	SOA formation from only anthropogenic VOC precursors with traditional partitioning theory
ANT-EP	Similar to ANT-T with enhanced partitioning efficiency toward aerosol phase
BIO-T	SOA formation from both biogenic and anthropogenic VOC precursors with traditional partitioning theory
BIO-ANT	Similar to BIO-T with isoprene emissions from anthropogenic sources
BIO-EP	Similar to BIO-ANT with enhanced partitioning efficiency toward aerosol phase
BIO-NT	Similar to BIO-ANT including the nighttime production of SOA from isoprene

Table 4. Comparison of observed and simulated OOA concentrations during MILAGRO experiment for the 5 sensitivity simulations listed in Table 3.

OOA ($\mu g/m^3$)	Urban station (T0)					Near-City station (T1)					Near-City station (PTP)				
	(ANT-T)	(ANT-EP)	(BIO-T)	(BIO-NT)	(BIO-EP)	(ANT-T)	(ANT-EP)	(BIO-T)	(BIO-NT)	(BIO-EP)	(ANT-T)	(ANT-EP)	(BIO-T)	(BIO-NT)	(BIO-EP)
Mean obs. ($\mu g/m^3$)			7.54					4.62					5.86		
Bias ($\mu g/m^3$)	−6.67	−5.61	−5.26	−4.91	−0.69	−4.44	−4.06	−3.66	−3.51	0.52	−5.4	−4.74	−4.37	−4.11	−0.17
RMSE ($\mu g/m^3$)	8.16	7.00	7.24	6.95	4.63	4.94	4.58	4.25	4.13	2.90	6.28	5.44	5.52	5.35	3.30
Correlation	0.56	0.63	0.35	0.37	0.50	0.18	0.23	0.16	0.18	0.17	0.50	0.64	0.03	0.05	0.32

The bias is computed as follow: $\text{Bias}(\mu g/m^3) = (1/N) \sum_i (M_i - O_i)$; the Root Mean Square Error is defined as: $\text{RMSE}(\mu g/m^3) = \sqrt{(1/N) \sum_i (M_i - O_i)^2}$; Where N is the number of samples, O_i are observations and M_i are model predictions. These indicators were computed on all OOA available data from the MILAGRO ground sites during March 2006.

a)

b)
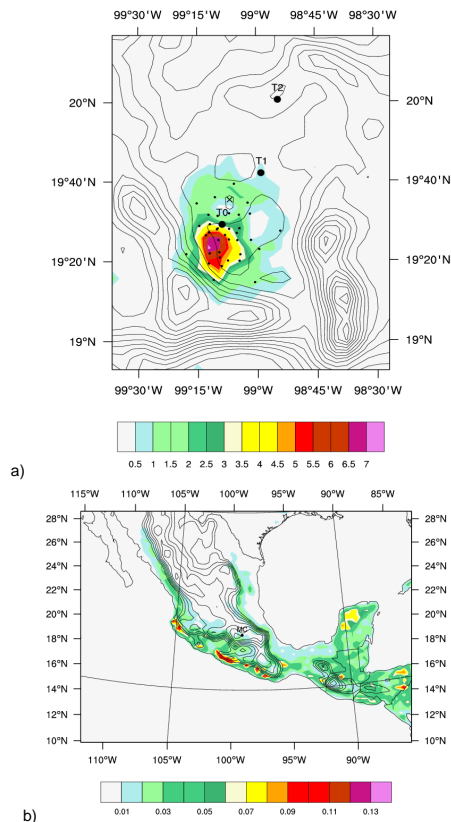
Fig. 1. CHIMERE geographical domains used over the Mexico region. Runs were performed at **(a)** fine (i.e. $5\times5\,km^2$) and **(b)** coarse (i.e. $35\times35\,km^2$) horizontal resolution respectively. The contours represent the distribution of emissions (Tons/km^2/day) averaged over 4–30 March 2006 period for (a) anthropogenic CO in the vicinity of the Mexico City and (b) regional isoprene estimates from the MEGAN model. The location of MILAGRO field campaign measurement sites used in this study including supersites (T0, T1, T2), mobile site of Pico de Tres Padres (PTP, cross north of T0) and RAMA monitoring air quality network (dots) are also included. Isocontours indicate the terrain height, with contours from 1 to 4 km. MC indicates the location of Mexico City.
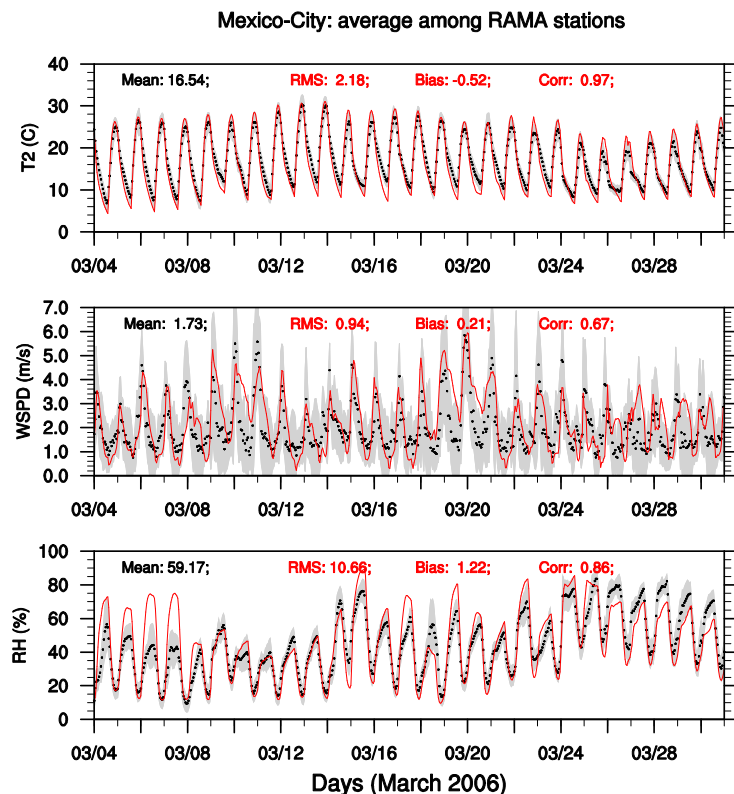
Fig. 2. Time series of meteorological variables (2 m-temperature, wind speed and relative humidity) simulated by the model (full line) and measured by RAMA network (dotted line) from 4 to 31 March 2006. 15 RAMA stations measuring meteorological data were available for this comparison.

ACPD

9, 12207–12281, 2009

Modeling organic aerosols during MILAGRO

A. Hodzic et al.

Title Page

Abstract   Introduction

Conclusions   References

Tables   Figures

◄◄   ►►

◄   ►

Back   Close

Full Screen / Esc

Printer-friendly Version

Interactive Discussion
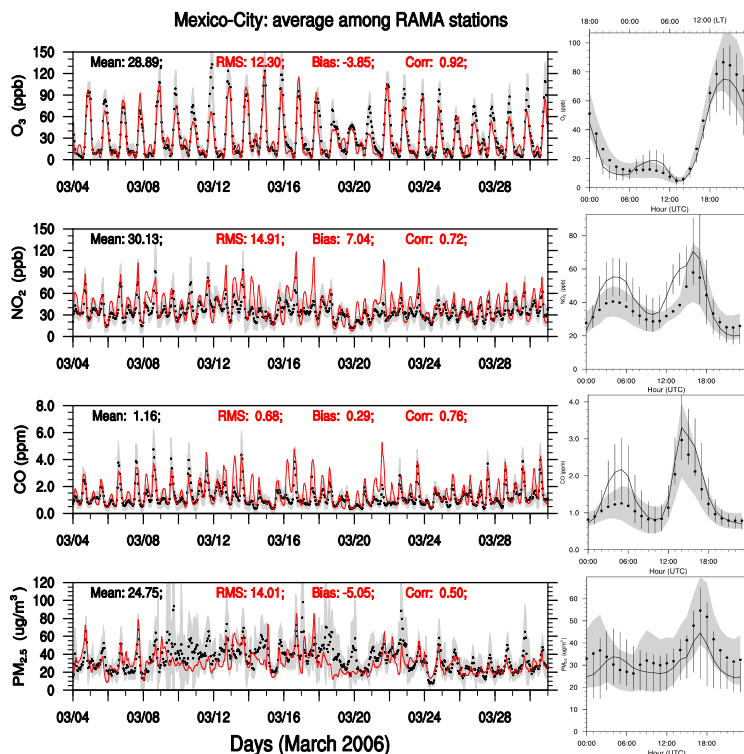
Figure 3

Fig. 3. Major pollutant concentrations as observed by air quality stations of the RAMA network (dotted line) and simulated by the CHIMERE model (full line, BIO-EP run) from 4 to 30 March 2006 (left panel). The variability among observations is denoted by gray shading and main statistical indicators for the comparison are also given (bias, RMSE and correlation). The right panel represents the corresponding diurnal cycles in UTC time for each pollutants averaged over all stations. The correspondence with the local time (LT=UTC−6 h) is also indicated on the upper x-axes. Model is solid line with error bars, observations are hourly points with shaded areas. All available measurements have been considered for this comparison (i.e. 21 ozone stations; 19 NO$_2$ stations; 25 CO stations, 8 PM$_{2.5}$ stations). The description of the RAMA network including the location of stations dedicate to the monitoring of each pollutant can be found at http://www.sma.df.gob.mx/simat/.
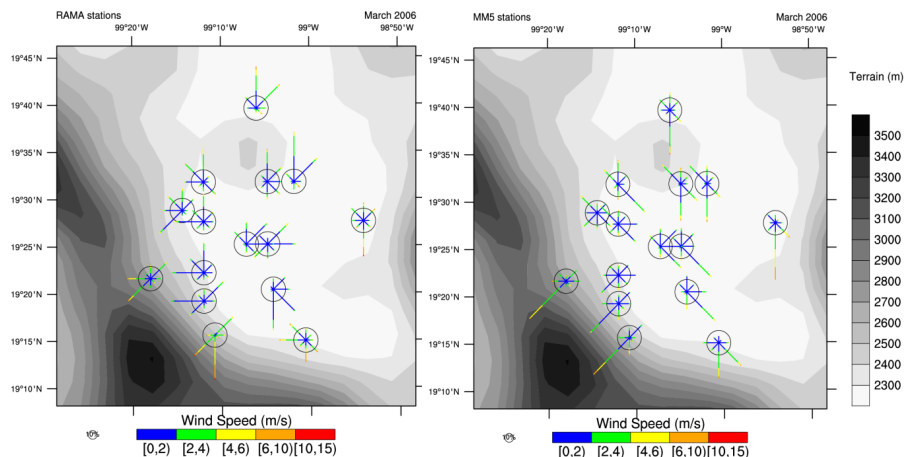
Fig. 4. Wind roses as predicted and observed at RAMA stations within the Mexico City basin indicating both the wind direction and the wind speed (m/s) during the MILAGRO experiment (i.e. 4–30 March 2006 period). The circle indicates the 10% occurrence. Winds appear to be generally weak and disorganized within the basin.

a) Mexico-City T0: 19.488N,-99.147W

Fig. 5a. Planetary boundary layer heights (PBLH) at the urban T0 site **(a)** as predicted by CHIMERE (full line) and observed by the radar wind profiler (dots). Daily averaged PBLH profiles are also displayed **(b)** for the T0 urban site (left panel), and the T1 near-urban location (right panel). Model predictions and variability are indicated by black solid line and vertical bars, while radar wind profiler observations and their variability are represented by black dots and shaded area. For T1, observations from radio soundings (diamonds) and lidar data (triangles) are also plotted when available. The 24 and 25 March undergo unstable, cloudy weather conditions. The correspondence with the local time (LT=UTC−6 h) is indicated on the upper x-axes of the diurnal profile plots.

12274

Title Page

Abstract | Introduction

Conclusions | References

Tables | Figures

◄◄ | ►►

◄ | ►

Back | Close

Full Screen / Esc

Printer-friendly Version

Interactive Discussion

b) Mexico-City T1: 19.703N,-98.982W

Fig. 5b. Planetary boundary layer heights (PBLH) at the urban T0 site **(a)** as predicted by CHIMERE (full line) and observed by the radar wind profiler (dots). Daily averaged PBLH profiles are also displayed **(b)** for the T0 urban site (left panel), and the T1 near-urban location (right panel). Model predictions and variability are indicated by black solid line and vertical bars, while radar wind profiler observations and their variability are represented by black dots and shaded area. For T1, observations from radio soundings (diamonds) and lidar data (triangles) are also plotted when available. The 24 and 25 March undergo unstable, cloudy weather conditions. The correspondence with the local time (LT=UTC−6 h) is indicated on the upper x-axes of the diurnal profile plots.

Fig. 6. Time series of modeled and observed surface concentrations ($\mu g\,m^{-3}$) of various carbonaceous compounds including total organic aerosol matter (TOA), primary organic aerosol (POA) and oxygenated organic aerosol (OOA). Comparison is made at the **(a)** urban site T0, and two near-urban sites **(b)** T1 and **(c)** PTP during the MILAGRO experiment. Black dots stand for observations, the red solid line for the ANT-T model run that accounts only for anthropogenic SOA precursors, and the green dashed line for the ANT-EP model run that examines the sensitivity to the enhanced partitioning towards aerosol phase. On the POA panel, black dots account for the measured POA from both anthropogenic and biomass burning sources, while blue dots indicate the primary organic mass that excludes organics generated by biomass burning emissions. Model results shown on the POA comparison panel includes also primary organic aerosols from biomass burning.
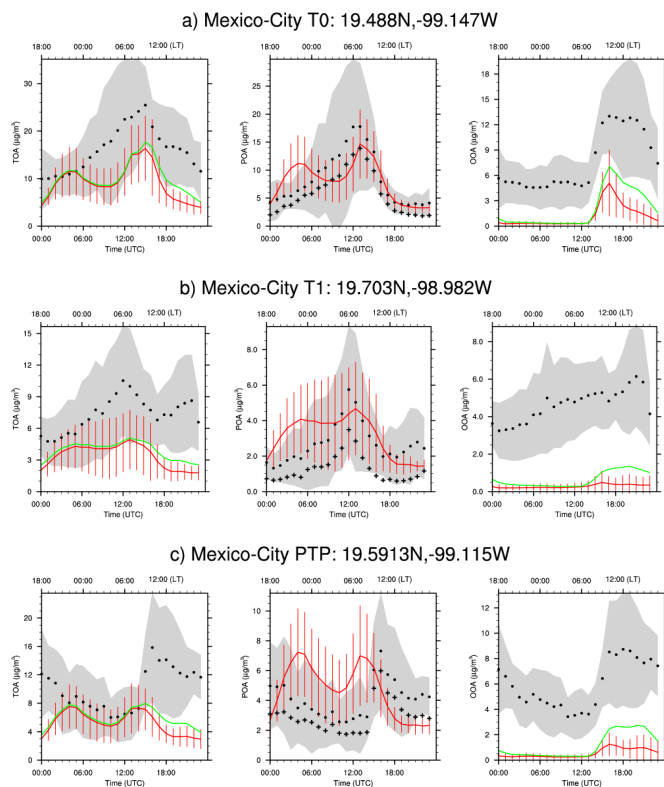
Fig. 7. Observed and predicted average diurnal profiles of total organic aerosol matter (TOA), primary organic aerosol (POA) and oxygenated organic aerosol (OOA) at T0 **(a)**, T1 **(b)**, and PTP **(c)** sites for the available MILAGRO dataset. Black dots and shaded area represent observations associated with their variability, the red solid line and red vertical bars indicate the ANT-T model run and the green solid line indicate the ANT-EP sensitivity simulation. Crosses shown on the POA plots indicate the primary organic mass that excludes organics generated by biomass burning emissions. Model results shown on the POA comparison panel include also primary organic aerosols from biomass burning. The correspondence with the local time (LT=UTC−6 h) is indicated on the upper x-axes.
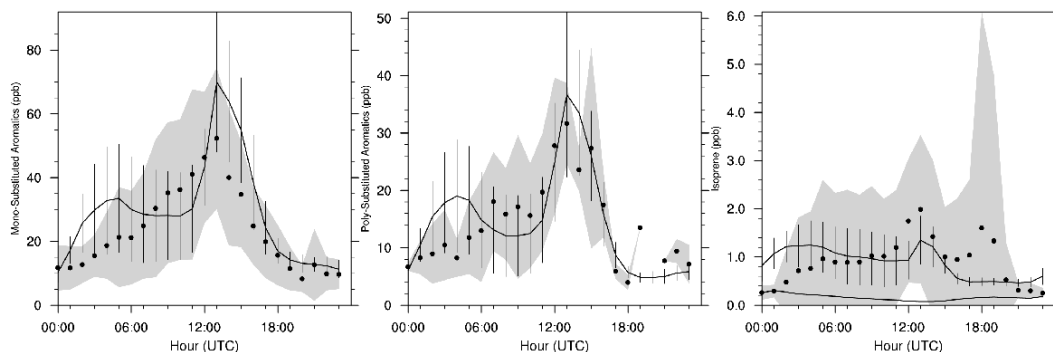
Fig. 8. Comparison of predicted (black dots) and observed (full line) surface concentrations of VOCs that are involved in the SOA formation including mono-substituted and poly-substituted aromatics and isoprene. Averaged diurnal cycles have been computed over the period of 4–30 March 2006 at the urban supersite (T0). The variability among observations and model predictions is denoted by gray shading and vertical bars respectively. The isoprene plot includes two model predictions: bottom full line represents biogenic isoprene emissions only (BIO-T run), while top line accounts for both biogenic and anthropogenic isoprene emissions (BIO-ANT run).
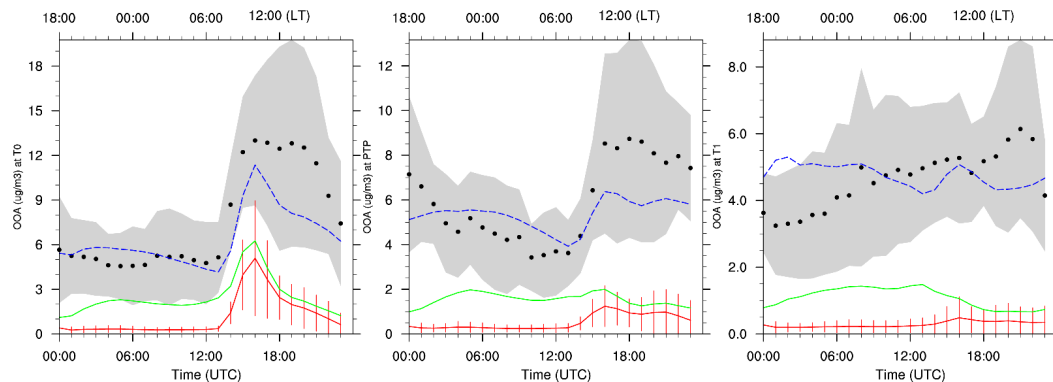
Fig. 9. Observed and predicted average diurnal profiles of OOA at T0, PTP and T1 sites during MILAGRO experiment. Black dots and shaded area represent observations associated with their variability, the red solid line and red vertical bars indicate the ANT-T model run, the green solid line indicate the BIO-T simulation, and blue dashed line the BIO-EP sensitivity simulation.

Full Screen / Esc

Printer-friendly Version

Interactive Discussion
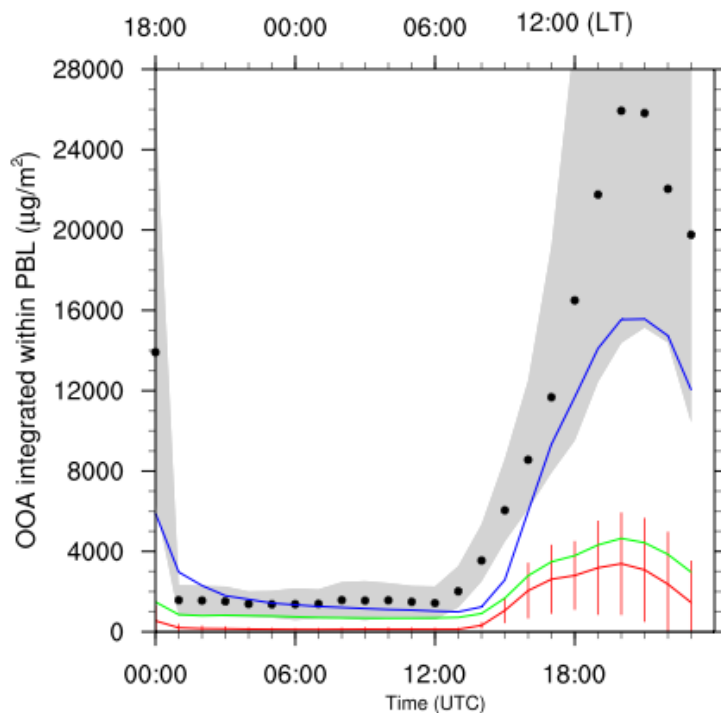
Fig. 10. Average diurnal profiles of column-integrated oxygenated organic aerosol (OOA, μg m^{-2}) within the boundary layer as observed and modeled during MILAGRO at T0. Similar to Fig. 10, black dots and shaded area represent observations associated with their variability, the red solid line and red vertical bars indicate the ANT-T model run, the green solid line indicate the BIO-T simulation, and blue dashed line the BIO-EP sensitivity simulation.
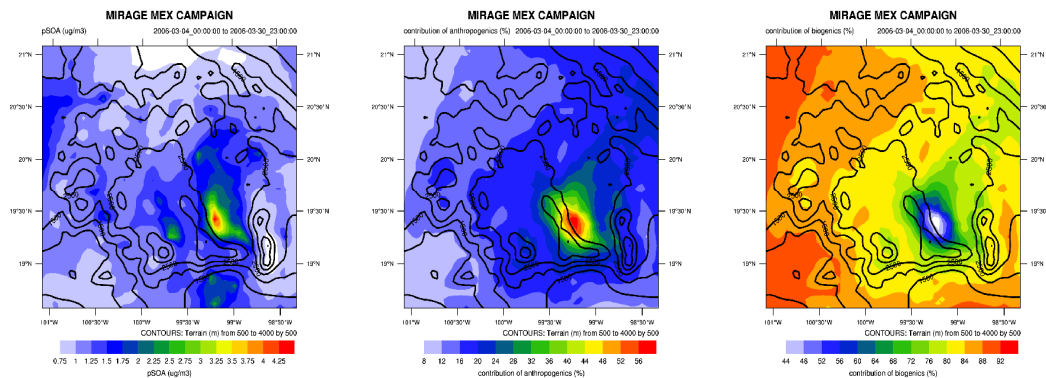
Fig. 11. Modeled SOA concentrations (μg×m^{-3}) for March 2006 based on BIO-T simulation **(a)**. Percentage contribution % to total SOA is shown for **(b)** anthropogenic emissions and (b) biogenic emissions.